CrystEngComm

Accepted Manuscript

ROYAL SOCIETY OF CHEMISTRY

www.rsc.org/crystengcomm

Cite this: DOI: 10.1039/c0xx00000x

www.rsc.org/xxxxxx

ARTICLE TYPE

Syntheses, characterizations and properties of nine novel Zn(Ⅱ) coordination polymers based on 4,4'-(phenylazanediyl)dibenzoic acid and various N-donor ligands

Lun Zhao*, Huadong Guo, Dong Tang , Min Zhang

Received (in XXX, XXX) Xth XXXXXXXXX 20XX, Accepted Xth XXXXXXXXX 20XX
DOI: 10.1039/b000000x

Nine novel coordination polymers, namely, $[ZnL(bpmp)_{0.5}]\cdot 3H_2O$ (**1**), $[Zn_2L_2(bibp)_2]\cdot H_2O$ (**2**), $[ZnL(bpp)]\cdot 7H_2O$ (**3**), $[Zn_2L_2(bidpe)_2]\cdot 2H_2O$ (**4**), $[Zn_3L_3(bpmp)_{0.5}\cdot(H_2O)_2]$ (**5**) $[ZnL(bibpip)_2]\cdot 3H_2O$ (**6**), [ZnL(bpmb)] (**7**), $[ZnL(bib)]\cdot DMF\cdot 4H_2O$ (**8**) and $[ZnL(bibp)]\cdot 2DMF$ (**9**) [H_2L = 4,4'-(phenylazanediyl)dibenzoic acid, bpmp = 1,4-bis(pyridin-4-ylmethl)piperazine, bibp = 4,4'-bis(imidazol-1-yl)biphenyl, bpp = 1,3-bis(4-pyridyl)propane, bidpe = 4,4'-bis(imidazol-1-yl)dipheny, bibpip = 1,4-bis(4-(1H-imidazol-l-yl)benzyl)piperazine, bpmb = 1,4-bis(pyridin-4-ylmethoxy)benzene and bib = 1,4-bis(imidazolyl)butane], have been synthesized under solvothermal and hydrothermal conditions. Their structures have been characterized by single-crystal X-ray diffraction analysis, elemental analysis, Infrared spectroscopy and thermogravimetric analysis. Compound **1** exhibits an infinite 3D structure with $\{4^4\cdot 6^{10}\cdot 8\}$ topology. Compound **2** features an unusual two-fold interpenetrating 3D framework with $\{3^{19}\cdot 4^{17}\cdot 5^9\}$ topology. Compound **3** shows the interweaving helical chains. Compound **4** views of 2-fold 1D chains are mutually interpenetrate each other from 2D sheets. Compound **5** exhibits an unusual 2D wave-like sheet. Compound **6** shows the 5-fold interpenetrating framework. Compound **7** displays a 1D chain. Compound **8** is also (4,4) layer structure which can be split into interesting helixes. Compound **9** shows the three-fold interpenetrating sheets are stacked in ABAB fashion and form a 3D framework. Their photochemical properties were measured.

Cite this: DOI: 10.1039/c0xx00000x

www.rsc.org/xxxxxx

ARTICLE TYPE

INTRODUCTION

Metal-Organic Frameworks(MOFs), also known as more specilized subgroup of coordination polymers (CPs), are made by linking inorganic and organic units by strong bonds(reticular synthesis)[1]. Careful selection of MOF constituents can yield crystals of ultrahigh porosity and high thermal and chemical stability. These materials contain functional pores to direct their specific and unique recognition of small molecules through several types of interactions: van der Waals interactions[2] of the framework surfaces with the substrate, metal−substrate interactions, and hydrogen bonding of the framework surface with the substrate[3]. These materials as a result of the high surface areas, tunable pore metrics, and high density of active sites within the very open structures, can be used to support homogeneous catalysts, stabilize short-lived catalysts, perform size selectivity, and encapsulate catalysts within their pores, offer many advantages to their use in catalysis[4]. These materials are composed entirely of strong bonds(e.g., C-C, C-H, C-O and M-O), they show high thermal stability ranging from 250° to 500°C[5]. At present, MOF chemistry has matured to the point where the composition, structure, functionality, porosity, and metrics of a metal organic structure can be designed for a specific application such as gas storage[6], separation[7], and sensing[8]. The chemistry and applications of MOFs have progressed substantially since their original inception more than decades ago[9]. To date, MOFs with permanent porosity are more extensive in their variety and multiplicity than any other class of porous materials. These aspects have made MOFs ideal candidates for storage of fuels(hydrogen[6a,10] and methane[11]), capture of carbon dioxide[12], catalysis applications[13], biological and medical applications[14], to mention a few. However, control-synthesizing MOFs and predicting their structures remain challenging. Proper organic bridging linkers are critical in constructing coordination polymers. 4,4'-(phenylazanediyl)dibenzoic acid (H_2L), which has advantages due to its different coordination modes lead to diverse multidimensional architectures[15]. In addition, a careful selection of N-donor ligands with different conformations as secondary auxiliary ligands, such as pyridine derivatives(bpp[16], bpmp[17], bpmb[18], bpp = 1,3-bis(4-pyridyl)propane, bpmp =1,4-bis(4-pyridin-4-ylmethyl)piperazine, bpmb = 1,4-bis(pyridine-4-ylmethoxy)benzene) and imidazole derivatives(bib[19], bibp[20], bidpe[21], and bibpip. bib = 1,4-bis(N-imidazolyl)butane, bib =1,4-bis(1-imidazolyl)benzene, bibp =1,4-bis(imidazol-1-yl)biphenyl, bidpe = 4,4'-bis(imidazol-1-yl)diphenyl ether, bibpip =1,4-bis(4-(1H-imidazol-1-yl)piperazine), is a key step for the rational design of structures with specific physical and chemical properties[22]. In our previous work, we have demonstrated that the rational selection of organic ligands with specific conformation and geometry is an effective approach to the construction of MOFs[23]. In this article, our research interest is focused on the design, synthesis and structural characterization of new coordination compounds with nitrogen donor ligands. H_2L was used to react with Zn(II) salts to fabricate nine new coordination polymers, i.e., $[ZnL(bpmp)_{0.5}]\cdot 3H_2O$**(1)**, $[Zn_2L_2(bibp)_2]\cdot H_2O$**(2)**, $[ZnL(bpp)]\cdot 7H_2O$ **(3)**, $[Zn_2L_2(bidpe)_2]\cdot 2H_2O$ **(4)**, $[Zn_3L_3(bpmp)_{0.5}\cdot(H_2O)_2]$ **(5)** $[ZnL(bibpip)_2]\cdot 3H_2O$ **(6)**, [ZnL(bpmb)] **(7)**, [ZnL(bib)] ·DMF·$4H_2O$ **(8)** and [ZnL(bibp)] ·2DMF **(9)**. The details of their syntheses, structures and properties are reported below.

Scheme 1 Molecular structure of ligands

Experimental section

Materials and methods

The H_2L was synthesized by 4,4'-dibromotriphenylamine and Copper(I) cyanide then hydrolyzing[24]. All other starting materials were of analytical grade and used as received without further purification. Elemental analyses (C, H, N) were performed with a Perkin-Elmer 240c elemental analyzer. Thermogravimetric analysis(TGA) was performed on a Perkin-Elmer TG-7 analyzer heated from 30 to 650 °C under nitrogen. The luminescent properties of these compounds were measured on a HITACHI F-7000 spectrometer. Powder X-ray diffraction (PXRD) data were recorded on a Rigaku D/M-2200T automated diffractometer (Figures S1-S9 in the supporting information). IR spectra were obtained from KBr pellets on a Perkin–Elmer 580B IR spectrometer in the 400-4000 cm^{-1} region.

Synthesis of $[ZnL(bpmp)_{0.5}]\cdot 3H_2O$ (1)

A mixture of $Zn(NO_3)_2\cdot 6H_2O$ (0.0297 g, 0.1 mmol), H_2L(0.0333 g, 0.1 mmol), bpmp (0.0268 g, 0.1 mmol), DMF (8 mL) and H_2O (2 mL) was placed in a Teflon reactor (20 mL) and heated at 80 °C for 3 days. After gradually cooling to room temperature at a rate of 10 °C h^{-1}, large quantities of colorless block crystals were obtained and the crystals were filtered off, washed with ethanol, and dried under ambient conditions. Yield of the reaction was 72% based on bpmp. Anal. calcd for $C_{28}H_{23}N_3O_7Zn$ (%): C, 58.10; H, 4.00; N, 7.26. Found: C, 57.94; H, 3.96; N, 7.22. FT-IR (4000–600 cm^{-1}): 3064 (w), 2775(w), 1681 (s), 1588 (s), 1488 (s), 1377 (s), 1141 (m), 1036(w), 1010 (m), 802 (w), 675 (m). 537(s).

Synthesis of $[Zn_2L_2(bibp)_2]\cdot H_2O$ (2)

A mixture of $Zn(NO_3)_2\cdot 6H_2O$ (0.0297 g, 0.1 mmol), H_2L(0.0333 g, 0.1 mmol), bibp (0.0286 g, 0.1 mmol), H_2O (10 mL) was placed in a Teflon reactor (20 mL) and heated at 160 °C for 3 days. After gradually cooling to room temperature at a rate of 20 °C h^{-1}, Large quantities of colorless block crystals were obtained and the crystals were filtered off, washed with ethanol, and dried under ambient conditions. Yield of the reaction was 61% based on bibp. Anal. calcd for $C_{76}H_{54}Zn_2N_{10}O_9$ (%): C, 66.04; H, 3.94; N, 10.13. Found: C,

65.64; H, 3.54; N, 10.48. FT-IR (4000–600 cm^{-1}): 3473 (w), 3133(m), 1596 (s), 1516 (s), 1311 (s), 1258 (s), 1060 (s), 962 (m), 822 (s), 781 (m), 655 (w), 647(m), 539.21(w).

Synthesis of [ZnL(bpp)]·$7H_2O$ (**3**)

A mixture of $Zn(NO_3)_2·6H_2O$ (0.0297 g, 0.1 mmol), H_2L(0.0333 g, 0.1 mmol), bpp (0.0198 g, 0.1 mmol), DMF (8 mL) and H_2O (2 mL) was placed in a Teflon reactor (20 mL) and heated at 80 °C for 3 days. After gradually cooling to room temperature at a rate of 10 °C h^{-1}, Large quantities of transparent block crystals were obtained and the crystals were filtered off, washed with ethanol, and dried under ambient conditions. Yield of the reaction was 63% based on bpp. Anal. calcd for $C_{33}H_{27}ZnN_3O_8$ (%): C,58.71; H, 4.03; N,6.22. Found: C, 59.42; H, 4.08; N, 6.30. FT-IR (4000–600 cm^{-1}): 3417 (w), 1671 (w), 1593 (s), 1376 (s), 1316 (m), 1014 (w), 782 (w).

Synthesis of [Zn_2L_2 (bidpe)$_2$] ·$2H_2O$ (**4**)

Compound **4** was prepared in the similar way as of **2** with bibp replaced by bidpe (0.0302 g,0.1 mmol). Large quantities of crystal-clear block crystals were obtained and the crystals were filtered off, washed with ethanol, and dried under ambient conditions. Yield of the reaction was 68% based on bidpe. Anal. calcd for $C_{76}H_{54}Zn_2N_{10}O_{12}$ (%): C, 63.83; H, 3.81; N, 9.80. Found: C, 64.13; H, 3.92; N, 9.91. FT-IR(4000–600 cm^{-1}): 3054 (w), 1592 (s), 1517 (s), 1312 (m), 1237 (s), 1063 (w), 834 (w), 784 (w), 709 (w), 655 (w).

Synthesis of [Zn_3L_3 (bpmp)$_{0.5}$ (H_2O)$_2$] ·H_2O (**5**)

Similarly, the procedure of preparing compound **5** is equal to the procedure of **4** by replacement of bibp by bpmp (0.0268 g, 0.1 mmol). Large quantities of colorless block crystals were obtained and the crystals were filtered off, washed with ethanol, and dried under ambient conditions. Yield of the reaction was 63% based on bpmp. Anal. calcd for $C_{136}H_{98}Zn_5N_{10}O_{28}$ (%): C, 61.70; H, 3.73; N, 5.29. Found: C, 61.54; H, 3.64; N, 5.33. FT-IR (4000–600 cm−1): 3063 (w), 1586 (s), 1489 (s), 1374 (s), 1175 (s), 1010 (w), 781 (s), 697 (s), 677 (m), 527 (m).

Synthesis of [ZnL(bibpip)$_2$]·DMF·$4H_2O$ (**6**)

Compound **6** was prepared in the same way as for Compound **1** by using bpmp to bibpip (0.0398 g, 0.1 mmol). Large quantities of transparent block crystals were obtained and the crystals were filtered off, washed with ethanol, and dried under ambient conditions. Yield of the reaction was 61% based on bibpip. Anal. calcd for $C_{92}H_{84}N_{16}O_{13}$ Zn_2 (%): C, 63.05; H,4.83; N, 12.79. Found: C, 62.60; H, 4.54; N, 11.69. FT-IR(4000–600 cm^{-1}): 3422 (w), 3100 (w), 2935 (w), 2805 (w), 1668 (m), 1594 (s), 1527 (m), 1372 (s), 1266 (m), 1068 (w), 843 (m), 782 (m), 660 (w).

Synthesis of [ZnL(bpmb)] **(7)**

Compound **7** was prepared in the similar way as of **2** with bibp replaced by bidpe to bpmb (0.0296 g, 0.1 mmol). Large quantities of colorless block crystals were obtained and the crystals were filtered off, washed with ethanol, and dried under ambient conditions. Yield of the reaction was 59% based on bpmb. Anal. calcd for $C_{58}H_{42}ZnN_4O_{10}$ (%): C,68.27; H, 4.15; N, 5.49. Found: C, 68.31; H, 4.12; N, 5.48. FT-IR (4000–600 cm^{-1}): 3133 (m), 1665 (s), 1593 (s), 1532 (s), 1489 (m), 1362 (s), 1313(s), 1279 (s), 1070 (s), 960 (m), 784 (s), 656(m).

Synthesis of [ZnL(bib)] ·DMF·$4H_2O$ (**8**)

Similarly, the procedure of preparing compound **1** is equal to the procedure of (4) by replacement of bpmp by bib (0.0190 g. 0.1 mmol). Large quantities of colorlessblock crystals were obtained and the crystals were filtered off, washed with ethanol, and dried under ambient conditions. Yield of the reaction was 68% based on bib. Anal. calcd for $C_{30}H_{26}ZnN_5O_4$ (%): C, 54.82; H, 4.60; N, 11.62. Found: C, 54.94; H, 4.54; N, 11.63. FT-IR (4000–600 cm^{-1}): 3130 (w), 1596 (s), 1505 (m), 1360 (s), 1110 (m), 1091 (m), 841 (w), 784 (m), 696 (w), 656 (m), 530(w).

Synthesis of [ZnL(bibp)] ·2DMF (**9**)

Compound **9** was prepared in the same way as for Compound **1** by using bpmp to bibp (0.0286 g, 0.1 mmol). Large quantities of colorless block crystals were obtained and the crystals were filtered off, washed with ethanol, and dried under ambient conditions. Yield of the reaction was 56% based on bibp. Anal. calcd for C_{44} $H_{36}N_7O_6Zn$ (%): C, 64.12; H, 4.40; N, 11.90. Found: C, 64.74; H, 4.64; N, 11.79. FT-IR (4000–600 cm^{-1}): 3137 (w), 1592 (s), 1518 (s), 1371 (s), 1173 (m), 1068 (m), 824 (w), 785 (m).

Scheme 2 Crystallographically established coordination modes of the carboxylic groups in compounds **1-9**

X-ray crystallography

Single-crystal XRD data for compounds 1 – 9 were recorded on a Bruker Apex CCD diffractometer with graphite-monochromatized Mo Kα radiation (λ = 0.71073 Å) at 165(2) K. Absorption corrections were applied using the multiscan technique. All the structures were solved by Direct Method of SHELXS-97[25] and refined by the full-matrix least-squares techniques by using the SHELXL-97[26] program within WINGX. No-hydrogen atoms were refined with anisotropic temperature parameters.The hydrogen atoms of the organic ligands were refined as rigid groups. Detailed crystallographic data and structure refinement parameters for **1-9** are summarized in Table 1.

Table 1. Crystal and Structure Refinement Data for Compounds **1-9**.

Results and discussion

Structure description of (1)

Compound **1** crystallizes in the monoclinic crystal system in space group C2/c. In the asymmetric unit, it contains an independent Zn(II)

cation, one L^{2-} ligand, a half of a bpmp ligand and three H_2O molecules (Fig. 1a). Coordination geometry for each Zn atom is a distorted octahedron with four O atoms from four different ligands forming the middle plane. One nitrogen atom and one Zn atom are in the axial position of the distorted octahedron. In this compound, the H_2L ligand acts as a "V-shape" link and the carboxylate group adopts a bismonodentate coordination mode (Scheme. 2a) to bridge two Zn centers to form paddlewheel $[Zn_2(CO_2)_4]$ clusters. The distance of Zn–Zn is 2.916(15) Å, Zn–O bond lengths are in the range of 2.022(3)–2.052(2) Å, and the Zn–N bond length is 2.024(2) Å[27,28]. All these distances and bond angles are within the normal range(Table S1 in the ESI†). Each L^{2-} ligand links two Secondary building units (SBUs) to form a 2D layered network (Fig. 1b), the rhombic lattice size is (22.798 Å× 16.584 Å). Then the bpmp ligand link the layers to further generate an infinite 3D framework (Fig. 1c). The dinuclear Zn(II) SBUs can be regarded as 6-connected nodes with the L ligand acting as linkers. A topology analysis reveals that the structure can be represented as the Schlafli symbol $\{4^4\cdot6^{10}\cdot8\}^{15}$, as displayed in (Fig. 1d).

Fig. 1 (a) Coordination environment of the Zn(II) ions in compound **1**. The hydrogen atoms are omitted for clarity. Symmetry codes: #1= -x+1.5, -y-0.5, -z+1; #2=-x+2, y-1, -z+1.5; #3= x, -y, z+0.5; #4=-x+2, -y+1, -z+1; #5=-x+2, y+1, -z+1.5; #6= x, -y, z-0.5. (b) views of 2D net structure. (c) views of the 3D framework. (d) The $\{4^4\cdot6^{10}\cdot8\}$ topology net.

Structure description of (2)

The crystal structure determination reveals that compound **2** crystallizes in the monoclinic crystal system in space group $P2_1/n$. The asymmetric unit contains two Zn(II) cations, one bibp ligand and two half of a bibp ligands, two deprotonated L^{2-} ligands and one H_2O molecule, which is omitted for clarity (Fig. 2a). In the asymmetric unit, the Zn(II) cation is coordinated by two carboxylic O atoms from two L^{2-} ligands and two nitrogen atoms from two bibp ligands to form a distorted tetrahedron geometry. In an asymmetric unit, the two carboxylate groups of the L^{2-} ligand take the same coordination modes. They all take a monodentate coordination mode (Scheme 2 b).The bond length of Zn-O bond distance vary in the range of 1.908(3)-1.975(3) Å and the Zn-N bond distance is 2.004(4)-2.030(4)Å. All these distances and bond angles are within the normal range(Table S1 in the ESI†). The bibp ligands connect Zn atoms to form a 1D chain. Then the L^{2-} ligands join all infinite 1D chains into a 3D framework. If L^{2-} and bibp are considered as linkers ,Zn(II) centers can be clarified as four-connected nodes. Thus, the topology of the structure can be simplified as a 3D framework of $\{3^{19}\cdot4^{17}\cdot5^9\}$ topology (Fig .2b). Because of the space nature of the single structure, two identical structure mutually interpenetrate each other into a 2-fold interpenetrated framework (Fig. 2c). The remaining vacuum space is occupied by some uncoordinated water molecules. Similar reports were found, but the result implies that the subtle difference in different solvents and decreased temperature rates has a great influence on the structure of the complexes.

Fig. 2 (a) Coordination environment of the Zn(II) ions in compound **2**. The hydrogen atoms are omitted for clarity. Symmetry codes: #1=x, y, z+1; #2=x-1, y, z-1; #3=x+1, y, z+1; #4=x, y, z-1; #5=-x+1, -y, -z; #6=-x-1, -y+1, -z+1. (b) views of 3D framework structure. (c) Schematic view of the two-fold interpenetrating framework.

Structure description of (3)

The crystal structure determination reveals that compound **3** crystallizes in the monoclinic crystal system in space group $C2/c$. The asymmetric unit contains one Zn(II) cation, one bpp ligand, one deprotonated L^{2-} ligand and seven H_2O molecule, which is omitted for clarity (Fig. 3a). In the asymmetric unit, the Zn(II) ions is coordinated by two carboxylic O atoms from two L^{2-} ligands and two nitrogen atoms from two bibp ligands to form a distorted tetrahedron geometry. In an asymmetric unit, the two carboxylate groups of the L^{2-} ligand take the same coordination modes. They all take a monodentate coordination mode (Scheme. 2b). The bond lengths of Zn-O bond distance vary in the range of 1.951(5)-1.955(4) Å, and the Zn-N bond distance is 2.045(5)-2.058(5) Å. All these distances and bond angles are within the normal range(Table S1 in the ESI†).

In the structure, neighboring Zn(II) atoms are connected by bpp ligands to generate 1D zigzag chains, the 1D zigzag chains are bridged by L^{2-} ligands into 2D sheets by the diagonal direction. If bpp and L^{2-} are considered as connecters, the Zn(II) centers can be clarified as four-connected nodes. Thus, the topology of the structure can be simplified as a (4,4) net the Schlafli symbol $\{4^2\cdot6^3\cdot8\}$ (Fig. 3b.c). The sheets are in ABAB stacked fashion and form a 3D framework(Fig. 3d).

Within the layer, there exists two 1D helical chains (-Zn(bpp)-Zn(bpp)-) running along the b axis, with a pitch of 18.709 Å based of the repeat unit of two bpp ligands and two Zn(II) motifs, and the other is $\{-L^{2-}$-Zn(bpp)- Zn-L^{2-}-Zn(bibp)- $L^{2-}\}$, with a pitch of 37.418 Å based of the repeat unit of two bpp ligands four Zn(II) and three L^{2-} motifs(Fig. 3g). Both of them exhibits the uniform hardness in one layer, the opposite hardness in the other layer(Fig. 3e, 3f, 3h).

Fig. 3 (a) Coordination environment of the Zn(II) ions in compound **3**. The hydrogen atoms are omitted for clarity. Symmetry codes: #1= x+, y-0.5, z; #2= -x+1.5, y-0.5, -z+0.5; #3=x-0.5, y+0.5, z; #4=-x+1.5, y+0.5, -z+0.5. (b, c) views of 2D net structure. (d) view of the sheets are stacked in ABAB fashion, a 3D framework. (e, f, g) views of the helical chains with uniform or opposite hardness. (h) views of the helical chains in the (4,4) layer.

Structure description of (4)

Compound **4** crystallizes in the triclinic crystal system in space group $P\bar{1}$. In the asymmetric unit, there exists two crystallographically unique Zn(II) atoms, two L^{2-} ligands, two bidpe ligands and two uncoordinated H_2O molecule. In the asymmetric unit, the Zn1 cation is

coordinated by two carboxylic O atoms from two L ligands and two nitrogen atoms from two bidpe ligands to form a distorted tetrahedron geometry; while the other Zn2 cation is coordinated by three carboxylic O atoms from two L^{2-} ligands and two nitrogen atoms from two bidpe ligands to form a distorted trigonal bipyramid environment(Fig. 4a). In the structure, there exists two L^{2-} ligands, which exhibit two different coordination modes, one the two carboxylate groups take the same coordination modes.They all take a monodentate coordination mode (Scheme 2b), the other, one carboxylate group takes a monodentate coordination mode to bridge Zn center while the other carboxylate group adopts a chelating in bidentate mode (Scheme 2d). The bond lengths of Zn-O bond distance vary in the range of 1.949(7)-2.410(6) Å and the Zn-N bond distance is 2.033(6)-2.050(5) Å. All these distances and bond angles are within the normal range(Table S1 in the ESI†).

Fig. 4 (a) Coordination environment of the Zn(II) ions in compound **4**. The hydrogen atoms are omitted for clarity. Symmetry codes: #1=x-1, y, z; #2= x+1, y, z. (b) views of the 1D chain. (c, d) views of 2-fold interpenetrated 1D chain. (e) views of the 2D sheets.

In the structure, neighboring two Zn(II) atoms are connected by two bidpe ligands to build a coordinative ring (Fig. 4a), These rings are combined together into a 1D chain by the L^{2-} ligands(Fig. 4b). Because of the large size of the rhombic channel (about 51.06 Å × 10.92 Å), two identical structures mutually interpenetrate each other into a 2-fold interpenetrated 1D chain(Fig. 4c, 4d). These 2-fold 1D chains are mutually interpenetrate each other from 2D sheets. Meanwhile, the sheets are stacked to form a 3D framework.

Structure description of (5)

The crystal structure determination reveals that compound **5** crystallizes in the orthorhombic crystal system in space group $P2_12_12$. The asymmetric unit contains three Zn(II) cations, which exhibits two different coordination geometries, as shown in Fig. 5a, the Zn1 cation is coordinated by two nitrogen atom from two bpmp ligand (Zn-N 2.045(6) Å) and two oxygen atoms from two L^{2-} ligand (Zn-O 1.958(5) Å) to complete a distorted tetrahedron geometry. The Zn2 cation is coordinated by four carboxylic O atoms from four L ligands(Zn-O 1.906(6)-1.948(6) Å) to form a distorted tetrahedron geometry. While the Zn3 cation exists in a distorted trigonal bipyramid geometry, being ligated by five oxygen atoms from three L^{2-} ligands and two H_2O molecules(Zn-O 1.973(5)- 2.387(10) Å). All these distances and bond angles is within the normal range (Table S1 in the ESI†). The L^{2-} anions adopt three coordinationn modes: the first connects three Zn centers through one bismonodentate and one monodentate (Scheme 2c); the second links two Zn centers via one monodentate carboxylate and one chelate carboxylate (Scheme 2d); the third the carboxylate group takes a μ_3-monodentate-bridging links two Zn centers (Scheme 2e). In this structure, Zn2 and Zn3 cations are coordinated by four L^{2-} ligands carboxylate groups and two oxygen atoms from H_2O molecular to form(SBU: $Zn_2(CO)_4(H_2O)_2$) clusters, the distance of Zn-Zn is 3.287 Å. The dinuclear Zn(II) SBU by two L^{2-} ligands connected two SBUs, meanwhile the SBU connected Zn1 by a L^{2-} ligands. The Zn1 atoms are connected by bpmp ligands to generate 2D wave-like sheets(Fig. 5c). The sheets are stacked fashion and formed a 3D framework. Within the framework, the O atoms(such as O1 or O2 in Fig. 5a) in uncoordinated carboxylate in the 2D sheets, exhibit a protruding arm to erect outer layer. Between O1 or O2 and the other uncoordinated carboxylic O atoms in the adjoining sheets(O1-O13 2.879 Å, O2-O13 3.176 Å), there exists a strong hydrogen bond interactions, which indicates the stability of the whole structure(Fig. 5d).

Fig. 5 (a) Coordination environment of the Zn(II) ions in compound **5**. The hydrogen atoms are omitted for clarity. Symmetry codes: #1=-x+1, -y, z; #2= x+0.5, -y+0.5, -z+2; #3=-x+2, -y, z; #4=x-0.5, -y+0.5, -z+2. (b) views of the 1D chain. (c) views of 2D wave-like sheets. (e) views of the 3D framework.

Structure description of (6)

The crystal structure determination reveals that compound **6** crystallizes in the triclinic crystal system in space group $P\bar{1}$. The asymmetric unit contains one Zn(II) cation, two half of a bibpip ligand, one deprotonated L^{2-} ligand and three H_2O molecules, which is omitted for clarity (Fig. 6a). In the asymmetric unit, the Zn(II) cation is coordinated by two carboxylic O atoms from two L^{2-} ligands and two nitrogen atoms from two bibpa ligands to form a distorted tetrahedron geometry. In an asymmetric unit, the two carboxylate groups of the L^{2-} ligands take the same coordination modes. They all take a monodentate coordination mode (Scheme. 2b).The bond lengths of Zn-O bond distance vary in the range of 1.908(3)-1.975(3) Å, and the Zn-N bond distance is 2.004(4)-2.030(4) Å. All these distances and bond angles are within the normal range(Table S1 in the ESI†). In the structure, neighboring Zn(II) atoms are connected by bibpa ligands to generate 1D zigzag chains, by the diagonal adjacent 1D zigzag chains are bridged by L^{2-} ligands into 2D wave-like sheets. If bibpa and L^{2-} are considered as connecters, the Zn(II) centers can be clarified as four-connected nodes. Thus, the topology of the structure can be simplified as a (4,4) net the Schlafli symbol $\{4^4\cdot6^2\}$ (Fig. 6d). Because of the space nature of the single net, five identical nets mutually interpenetrate each other form a 5-fold interpenetrate framework (Fig. 6e).

Fig. 6 (a) Coordination environment of the Zn(II) ions in compound **6**. The hydrogen atoms are omitted for clarity. Symmetry codes: #1=-x+1, -y, -z+2; #2=-x+2, -y+2, -z+1; #3=x-1, y+1, z; #4=x+1, y-1, z; #5=-x+1, -y+1, -z. (b, c, d) views of 2D wave-like sheets. (e) Schematic view of the 5-fold interpenetrating framework.

Structure description of (7)

Compound **7** crystallizes in the monoclinic crystal system in space group $C2/c$. The asymmetric unit contains one Zn(II) cation, one

bpmb ligand, one deprotonated L^{2-} ligand(Fig. 7a). In the asymmetric unit, the Zn(II) ions is coordinated with two carboxylic O atoms from two HL^- ligands and two nitrogen atoms from two bpmb ligands, the unit adopts a distorted tetrahedron geometry. In an asymmetric unit, the one carboxylate group of H_2L ligand takes a monodentate coordination mode (Scheme. 2f). The bond lengths of Zn-O bond and the Zn-N bond are 1.977(3) Å and 2.043(3) Å, separately. All these distances and bond angles are within the normal range(Table S1 in the ESI†).

In the structure, neighboring Zn(II) atoms are connected by bpmb ligands to generate 1D zigzag chains, the HL^- ligand act as a terminal ligand to coordinate with one Zn(II) atom by monodentate coordination mode (Fig. 7b). The 1D zigzag chains are mutually interpenetrate each other shaping 2D sheets (Fig. 7c). Because of existing no coordinate carboxylic O atoms in the 1D zigzag chain, there are hydrogen bond interactions between the uncoordinated carboxylic O atom and the other uncoordinated carboxylic O atoms of the other chain in the adjoining layer. Within this framework, the distance between two O atoms belong to different layers is 2.628 Å, which promotes the stability of the structure(Fig. 7d).

Fig. 7 (a) Coordination environment of the Zn(II) ions in compound **7**. The hydrogen atoms are omitted for clarity. Symmetry codes: #1=-x+1.5, -y+3.5, -z+2; #2=-x+1, y, -z+1.5. (b) views of the 1D chain. (c) views of 2D sheets. (d) views of the distances between two O atoms.

Structure description of (8)

Compound **8** crystallizes in the Orthorhombic crystal system in space group *Pbca*. The asymmetric unit contains one Zn(II) cation, two half of one bib ligand, one deprotonated L^{2-} ligand, one DMF molecule, and four H_2O molecule, which is omitted for clarity (Fig. 8a). In the asymmetric unit, the Zn(II) cation is coordinated by two carboxylic O atoms from two L^{2-} ligands and two nitrogen atoms from two bib ligands to form a distorted tetrahedron geometry. In an asymmetric unit, the two carboxylate groups of the L^{2-} ligand take the same coordination modes. They all take a monodentate coordination mode (Scheme. 2b). The bond lengths of Zn-O bond vary in the range of 1.970(5)-1.996(5) Å and the Zn-N bond distance is 1.991(6)-2.042(7) Å. All these distances and bond angles are within the normal range(Table S1 in the ESI†). In this structure, neighboring Zn(II) atoms are connected by bib ligands to generate 1D zigzag chains, the diagonal adjacent 1D zigzag chains are bridged by L^{2-} ligands into 2D wave-like sheets. If bip and L^{2-} are considered as connecters, the Zn(II) centers can be clarified as four-connected nodes. Thus, the topology of the structure can be simplified as a (4,4)net (Fig. 8b, 8c). The sheets are stacked fashion and form a 3D framework. Within the layer, there exists 1D helical chains (-L^{2-}-Zn(bib)-Zn(bib)-) running along the b axis, with a pitch of 14.245 Å based of the repeat unit of one L^{2-} and two $[Zn(bib)]^{2+}$ motifs (Fig. 8d). In each layer, the adjoining helical chains exhibit the opposite hardness (Fig. 8d).

Fig. 8 (a) Coordination environment of the Zn(II) ions in compound **8**. The hydrogen atoms are omitted for clarity. Symmetry codes: #1=-x+2, -y, -z; #2= -x+2, -y+1, -z; #3=x, -y+0.5, z-0.5; #4=x, -y+0.5, z+0.5, #5=-x+1, y-0.5, -z-0.5; #6=-x+1, y+0.5, -z-0.5. (b, c) views of 2D net structure. (d) A view of the helical chains.

Structure description of (9)

The crystal structure determination reveals that compound **9** crystallizes in the monoclinic crystal system in space group $P2_1/c$. The asymmetric unit contains one Zn(II) cation, one deprotonated L^{2-} ligand, one bibp ligand, and two DMF molecules which is omitted for clarity (Fig. 9a). In the asymmetric unit, the Zn(II) cation is coordinated by two carboxylic O atoms from two L^{2-} ligands and two nitrogen atoms from two bibp ligands to form a distorted tetrahedron geometry. In an asymmetric unit, the two carboxylate groups of the L^{2-} ligand take the same coordination modes. They all take a monodentate coordination mode (Scheme. 2b). The length of Zn-O bond vary in the range of 1.960(6)-1.961(5) Å and the Zn-N bond distance is 2.007(6)-2.048(7) Å. All these distances and bond angles are within the normal range(Table S1 in the ESI†). The bibp ligand connect Zn atoms to form a 1D chain. The L^{2-} ligands then join all infinite 1D chains into a 2D sheets. If L^{2-} and bibp are considered as linkers, Zn(II) centers can be clarified as four-connected nodes(Fig. 9b). Thus, the topology of the structure can be simplified as a (4,4) net (Fig. 9c).

Because of the space nature of the single structure, three identical structure mutually interpenetrate each other into a 3-fold interpenetrated sheets (Fig. 9d). The 3-fold interpenetrated sheets are in ABAB stacked fashion and form a 3D framework (Fig. 9e). Within the layer, there exists 1D helical chains (-L^{2-}-Zn(bibp)- L^{2-}-Zn(bibp)-) running along the z axis, with a pitch of 14.160 Å based of the repeat unit of one L^{2-} and one $[Zn(bibp)]^{2+}$ motifs. In each layer, the adjoining helical chains exhibit the opposite hardness (Fig. 9f).

Fig. 9 (a) Coordination environment of the Zn(II) ions in compound **9**. The hydrogen atoms are omitted for clarity. Symmetry codes: #1=x+1, y, z+1; #2= x-1, -y+0.5, z+0.5; #3=x+1, -y+0.5, z-0.5; #4=x-1, y, z-1. (b, c) views of 2D net structure. (d) Schematic view of the three-fold interpenetrating sheets. (e) The sheets are stacked in ABAB fashion and form a 3D framework. (f) A view of the helical chains.

Thermal Analysis. To characterize the thermal stabilities of compounds **1-9**, their thermal behaviors were investigated by TGA (Fig. 10). The experiments were performed on samples consisting of numerous single crystals of **1-9** under nitrogen atmosphere with a heating rate of 10°C/min. For **1**, the destruction of the framework occurs at ca. 375°C. The remaining weight corresponds to the formation of ZnO (obsd 14.7%, calcd 14.1%). Compound **2** remains stable up to ca. 350°C, finally leading to the formation of the stoichiometric amount of ZnO as residue (obsd 12.3%, calcd 11.78%). For **3**, the decomposition of the compound occurs at ca. 280°C, and the remaining weight corresponds to the formation of ZnO (obsd 12.6%, calcd 12.2%). Compound **4** is stable up to ca. 375°C with the remaining residue of ZnO (obsd 11.1%, calcd 11.5%). For **5**, the departure of organic ligand occurs at ca. 300°C and the remaining

weight corresponds to the formation of ZnO(obsd 16.9%, calcd 15.4%). For **6**, the departure of organic ligand occurs at ca. 310°C and the remaining weight corresponds to the formation of ZnO(obsd 10.2%, calcd 9.29%). For **7**, the departure of organic ligand occurs at ca. 350°C and the remaining weight corresponds to the formation of ZnO (obsd 9.11%, calcd 8.0 %). For **8**, the decomposition of the compound occurs at ca. 300°C and the remaining weight corresponds to the formation of ZnO(obsd 12.2%, calcd 11.3%). For **9**, the decomposition of the compound occurs at ca. 350°C and the remaining weight corresponds to the formation of ZnO(obsd 12.9%, calcd 9.9%).

Fig.10 The TGA diagrams of complexes **1-9**.

Photoluminescence Properties. Because of excellent luminescent properties of d^{10} metal coordination polymers, the luminescent properties of compound **1-9** were investigated in the solid state at room temperature. As shown in Fig. 11. The emission peaks at 424 nm for L(λ_{ex}=396nm). the emission peaks were at 408 nm in compound **1** (λ_{ex} =369nm), 410 nm in compound **2** (λ_{ex} =338nm), 412 nm in compound **3** (λ_{ex} =369nm), 433 nm in compound **4** (λ_{ex} =357nm), 450 nm in compound **5** (λ_{ex} =397nm), 420 nm in compound **6** (λ_{ex} =377nm), 418nm in compound **7** (λ_{ex} =371nm), 430 nm in compound **8** (λ_{ex} =372nm) and 420 nm in compound **9** (λ_{ex} =373nm). These emissions can probably be assigned to the intraligand (π–π* or π*–n) fluorescent emission within the molecular orbital manifolds of the N-donor moieties and phenyl rings of L moieties. These compounds may be suitable as excellent candidates for blue-fluorescent materials, since they are highly thermally stable and insoluble in common solvents.

Particular attention should be paid to Compound **3**, which exhibits an intense emission with a maximum at 412 nm upon excitation at 369 nm, its emission characteristics are similar to those of the L ligand but shows an obvious blue shift of 12 nm as compared with that of the L ligand. The phenomenon is probably caused by a change in the HOMO and LUMO energy levels of the deprotonated L^{2-} anions and neutral ligands coordinating to the Zn(II) centers, a charge-transfer transition between ligands and metal centers, and a joint contribution of the intraligand transitions or charge-transfer transitions between the coordinated ligands and the metal centers[29]. In addition, the blue shift is also attributed to the non-coplanar ligands and the different distortion among the benzene rings, which prevent the efficient electron transfer in compound **3**[15].

Fig. 11 The solid-state photoluminescent spectra of **1-9** and H_2L at room temperature.

Conclusions

In this study, nine new coordination polymers with novel architectures have been synthesized successfully under hydrothermal conditions with different solvents and decreased temperature rates by using the flexible carboxylic acid and the various N-donor ligands as auxiliary ligands. Their structural differences indicate that the solvothermal conditions and the reaction temperature have remarkable influence on the resultant topologies. The results also show that the flexible carboxylic acid is good candidates for the construction of high dimensional MOFs. These nine compounds not only fill the aesthetic diversity of coordinative network chemistry, but also may provide a potential way for the selective design of versatile network-based materials. The photoluminescent behaviors show that these complexes may be good candidates for optical materials.

Acknowledgements

This work was financially supported by the Program of the 12th Five Science and Technology Research of Jilin Province Department of Education (No. 2013248).

Notes and references

Notes

The authors declare no competing financial interest.

Department of Chemistry, Changchun Normal University, Changchun, 130032, P. R. China. E-mail:zhaolun7511@126.com; Fax: +86-431-86168903; Tel: +86-431-86168903

† Electronic Supplementary Information (ESI) available: Crystallographic data in CIF format, selected bond lengths and angles, and XRD. CCDC: [1058540. 1058542.1058543.1058545-1058548. 1058550. 10585551]. For ESI and Crystallographic data in CIF format or other electronic format See DOI: 10.1039/b000000x/

[1](a)Q. L. Zhu and Q. Xu, *Chem. Soc. Rev*., 2014, **43**, 5468; (b)W. G. Lu, Z. W. Wei, Z. Y. Gu, T. F. Liu, J. Park, J. Park, J. Tian, M. W. Zhang, Q. Zhang, T. Gentle, M. Bosch and H. C. Zhou, *Chem. Soc. Rev.,* 2014, **43**, 5561; (c)H. Furukawa, K. E. Cordova, M. O'Keeffe and O. M. Yaghi, *Science*. 2013, **341**, 974; (d)M. Kurmoo, *Chem. Soc. Rev.,* 2009, **38**, 1353; (e)S. Kitagawa and R. Matsuda, *Coord. Chem. Rev.,* 2007, **251**, 2490; (f); (g)S. T. Meek, J.A. Greathouse and M. D. Allendorf, *Adv. Mater.,* 2011, **23**, 249; (h)S. Kitagawa, R. Kitaura and S. Noro, Angew. Chem. Int. Ed., 2004, **43**, 2334; (i)S. L. James, *Chem. Soc. Rev.,* 2003, **32**, 276.

[2](a) S. Zuluaga, P. Canepa, K. Tan, Y. J. Chabal and T. Thonhauser, *J. Phys.: Condens. Matter*, 2014, **16**, 133002; (b)H. Isla, E. M. Perez and N. Martin, *Angew. Chem. Int. Ed.,* 2014, **53**, 5629; (c)B. L. Chen, S. C. Xiang and G. D. Qian, *Acc. Chem. Res.,* 2010, **43**, 1115; (d)D. C. Langreth, B. I. Lundqvist, S. D. Chakarova-Kack, V. R. Cooper, M. Dion, P. Hyldgaard, A. Kelkkanen, J. Kleis, L. Z. Kong, S. Li, P. G. Moses, E. Murray, A.

Puzder, H. Rydberg, E, Schroder and T. Thonhauser, *J. Phys.: Condens. Matter,* 2009, **21**, 084203; (e)S. Keskin, J. C. Liu, R. B. Rankin, J. K. Johnson and D. S. Sholl, *Ind. Eng. Chem. Res.,* 2009, **48**, 2355; (f)R. Custelcean and B. A. Moyer, *Eur. J. Inorg. Chem.,* 2007, **10**, 1321.

[3](a)N. A. Khan, Z. Hasan and S. H. Jhung, *J. Harzard Mater.,* 2013, **244**, 444; (b)R. M. Yu, X. F. Kuang, X. Y. Wu, C. Z. Lu and J. P. Donahue, *Coord. Chem. Rev.,* 2009, **253**, 2872; (c)L. F. Ma, L. Y. Wang, J. L. Hu, Y. Y. Wang and G. P. Yang, *Cryst. Growth Des.,* 2009, **9**, 5334; (d)R. L. LaDuca, *Coord. Chem. Rev.,* 2009, **253**, 1759; (e)X. J. Jiang, S. Z. Zhang, X. G. Wang, J. S. Li and M. Du, *CrystEngComm,* 2009, **11**, 855; (f)R. Custelcean and B. A. Moyer, *Eur. J. Inorg. Chem.,* 2007, **10**, 1321; (g)J. L. C. Rowsell, O. M. Yaghi, *Micropor. Mesopor. Mat.,* 2004, **73**, 3.

[4](a)C. C. Wang, J. R. Li, X. L. Lv, Y. Q. Zhang and G. S. Guo, *Engergy Environ. Sci.,* 2014, **7**, 2831; (b)K. Leus, Y. Y. Liu, P. Van Der Voort, *Catal. Rev.,* 2014, **56**, 1; (c)J. Y. Lee, O. K. Farha, K. A. Scheidt, S. B. T. Nguyen and J. T. Hupp, *Chem. Soc. Rev.,* 2009, **38**, 1450; (d)D. Farrusseng, S. Aguado and C. Pinel, *Angew. Chem. Int. Ed.,* 2009, **48**, 7502.

[5](a)M. Eddaoudi, J. Kim, N. Rosi, D. Vodak, J. Wachter, M. O'Keeffe and O. M. Yaghi, *Science*, 2002, **295**, 469; (b) K. S. Park, Z. Ni, A. P. Cote, J. Y. Choi, R. D. Huang, F. J. Uribe-Romo, H. K. Chae, M. O'Keeffe and O. M. Yaghi, *Proc. Natl. Acad. Sci. U.S.A.* 2006, **103**, 10186.

[6](a)Y. B. He, B. Li, M. O'Keeffe and B. L. Chen, *Chem. Soc. Rev.,* 2014, **43**, 5618; (b)M. Alhamami, H. Doan and C. H. Cheng, *Materials*, 2014, **7**, 3198; (c)A. Uzun and S. Keskin, *Prog. Surf. Sci.,* 2014, **89**, 56; (d)A. Morozan and F. Jaouen, *Energy Environ. Sci.,* 2012, **5**, 9269; (e)S. Q. Ma and H. C. Zhou, *Chem. Commun.,* 2010, **46**, 44; (f)K. M. Thomas, *Dalton Trans.,* 2009, **9**, 1487; (g)R. J. Kuppler, D. J. Timmons, Q. R. Fang, J. R. Li, T. A. Makal, M. D. Young, D. Q. Yuan, D. Zhao, W. J. Zhuang and H. C. Zhou, *Coord. Chem. Rev.,* 2009, **253**, 3042;

[7](a)Z.R. Herm, E.D. Bloch, J.R. Long, *Chem. Mater.,* 2014, **26**, 323; (b)B. Van de Voorde, B. Bueken, J. Denayer and D. De Vos, *Chem. Soc. Rev.,* 2014, **43**, 5766; (c)B. Li, H. L. Wang and B. L. Chen, *Chem-Asian J.*, 2014, **9**, 1474; (d)Q.Y. Yang, D.H. Liu, C.L. Zhong and J. R. Li, *Chem. Rev.,* 2013, **113**, 8261; (e)J. R. Li, J. Sculley, H. C. Zhou, *Chem. Rev.,* 2012, **112**, 869; (f)Z. Y. Gu, C. X. Yang, N. Chang and X. P. Yan, *Acc. Chem. Res.,* 2012, **45**, 734; (g)J. R. Li, Y. G. Ma, M. C. McCarthy, J. Sculley, J. M. Yu, H. K. Jeong, P. B. Balbuena and H. C. Zhou, *Coord. Chem. Rev.,* 2011, **255**, 1791; (h)J. R. Li, R. J. Kuppler and H. C. Zhou, *Chem. Soc. Rev.,* 2009, **38**, 1477.

[8](a)J. P. Lei, R. C. Qian, P. H. Liang and H. X. Ju, *Trac-Trend. Anal. Chem.,* 2014, **58**, 71; (b)C. M. Doherty, D. Buso, A. J. Hill, S. Furukawa, S. Kitagawa and P. Falcaro, *Acc. Chem. Res.,* 2014, **47**, 396; (c)J. Rocha, L. D. Carlos, F. A. Almeida and D. Ananias, *Chem. Soc. Rev.,* 2011, **40**, 926; (d)J. Della Rocca and W. B. Lin, *Eur. J. Inorg. Chem.,* 2010, **24**, 3725; (e)L. E. Kreno, K. Leong, O. K. Farha, M. Allendorf, R. P. Van Duyne and J. T. Hupp, *Chem. Rev.,* 2012, **112**, 1105.

[9](a) R. Robson, *Dalton Trans.,* 2008, 5113; (b)O. M. Yaghi, G. M. Li and H. L. Li, *Nature*, 1995, **378**, 703; (c) O. M. Yaghi and H. L. Li, *J. Am. Chem. Soc.,* 1995, **117**, 10401; (d)B. F. Hoskins and R. Robson, *J. Am. Chem. Soc.,* 1990, **112**, 1546; (e) B. F. Hoskins and R. Robson, *J. Am. Chem. Soc.,* 1989, **111**, 5962; (f)J.C., Jr Bailar, *Prep. Inorg. React.,* 1964, **1**, 1.

[10](a)M. P. Suh, H. J. Park, T. K. Prasad and D. W. Lim, *Chem. Rev.,* 2012, **112**, 782; (b)J. Sculley, D. Q. Yuan and H. C. Zhou, *Energy Environ. Sci.,* 2011, **4**, 2721; (c)Y.H. Hu and L. Zhang, *Adv. Mater.,* 2010, **22**, e117; (d)L. J. Murray, M. Dinca and J. R. Long, *Chem. Soc. Rev.*, 2009, 38, 1294; (e)N. L. Rosi, J. Eckert, M. Eddaoudi, D. T. Vodak, J. Kim, M. O'Keeffe and O. M. Yaghi, *Science,* 2003, **300**, 1127.

[11](a)Y. B. He, W. Zhou, G.D. Qian and B. L. Chen, *Chem. Soc. Rev.,* 2014, **43**, 5657; (b)J. A. Mason, M. Veenstra and J. R. Long, *Chem. Sci.,* 2014, **5**, 32; (c) Y. Peng, V. Krungleviciute, I. Eryazici, J. T. Hupp, O. K. Farha and T. Yildirim, *J. Am. Chem. Soc.,* 2013, **135,** 11887; (d)R. B. Getman, Y. S. Bae, C. E. Wilmer and R. Q. Snurr, *Chem. Rev.,* 2012, **112**, 703; (e)D. Zhao, D. J. Timmons, D. Q. Yuan and H. C. Zhou, *Acc. Chem. Res.,* 2011, **44**, 123.

[12](a) J. Zhao, W. W. Dong, Y. P. Wu, Y. N. Wang, C. Wang, D. S. Li and Q. C. Zhang, *J. Mater. Chem. A*, 2015, **3**, 6962; (b)R. Sabouni, H. Kazemian, S. Rohani, *Environ. Sci. Pollut. R.,* 2014, **21**, 5427; (c) B. Liu, J. T. Shi, K. F. Yue, D. S. Li and Y. Y. Wang, *Cryst. Growth Des.,* 2014, **4**, 2003; (d) R. Matsuda, Bull. Chem. Soc. Jpn., 2013, **86**, 1117; (e) K. Sumida, D. L. Rogow, J. A. Mason, T. M. McDonald, E. D. Bloch, Z. R. Herm, T. H. Bae and J. R. Long, *Chem. Rev.,* 2012, **112**, 724; (f) J. Liu, P. K. Thallapally, B. P. McGrail, D. R. Brown and J. Liu, *Chem. Soc. Rev.,* 2012, **41**, 2308.

[13](a) M. Zhao, S. Ou and C. D. Wu, *Acc. Chem. Res.,* 2014, **47**, 1199; (b)S. Nakagaki, G. K. Baio Ferreira, G. M. Ucoski and K. A. Dias de Freitas, *Molecules.,* 2013, **18**, 7279; (c) A. Dhakshinamoorthy, M. Opanasenko, J. Cejka and H. Garcia, *Catal. Sci. Technol.,* 2013, **3**, 2509; (d) M. Yoon, R. Srirambalaji and K. Kim, *Chem. Rev.,* 2012, **112**, 1196; (e) M. Ranocchiari and J. A. van Bokhoven, *Phys. Chem. Chem. Phys.,* 2011, **13**, 6388; (f) A. Corma, H. Garcia and F. X. L. I. Llabres I Xamena, *Chem. Rev.,* 2010, **110**, 1606; (g) D. Farrusseng, S. Aguado and C. Pinel, *Angew. Chem. Int. Ed.,* 2009, **48**, 7502.

[14](a)J. H. Jung, J. H. Lee, J. R. Silverman and G. John, *Chem. Soc. Rev.,* 2013, 42, 924; (b)C. Y. Sun, C. Qin and Z. M. Su, *Expert Opin. Drug Del.,* 2013, **10**, 89; (c) P. Horcajada, R. Gref, T. Baati,P. K. Allan, G. Maurin, P. Couvreur, G. Ferey, R. E. Morris and C. Serre, *Chem. Rev.,* 2012, **112**, 1232; (d) A. C. McKinlay, R. E. Morris, P. Horcajada, G. Ferey, R. Gref, P. Couvreur and C. Serre, *Angew. Chem. Int. Ed.,* 2010, **49**, 6260.

[15]J. L. Zhou, Y. Y. Wang, L. Qin, M. D. Zhang, Q. X. Yang and H. G. Zheng, *CrystEngComm.*, 2013, **15**, 616.

[16](a)B. Lesniewska, F. Perret, K. Suwinska and A. W. Coleman, *CrystEngComm.*, 2014, **16**, 4399; (b)B. Xu, Q. S. Liang, L. T. Liu, Q. S. Liu and C. C. Li, *RSC Adv.,* 2014, **4**, 13919; (c)J. Gu, X. E. Jiang, Z.H. Su, Z. F. Zhao and B. B. Zhou, *Inorg. Chim. Acta.*, 2013, **400**, 210; (d)K. Fukuhara, S. I. Noro, K. Sugimoto, T. Akutagawa, K. Kubo and T. Nakamura, *Inorg. Chem.,* 2013, **52**, 4229; (e)Y. E. Cha, X. Li, X. Ma, C. Q. Wan, X. B. Deng and L. P. Jin, *CrystEngComm.,* 2012, **14**, 5322.

[17](a)B. Xu, Y. Q. Sun, J. Li and C. C. Li, *RSC Adv.,* 2014, **4**, 25588; (b)J. J. Shen, M. X. Li, Z. X. Wang, S. R. Zhu, M. Shao and X. He, *Inorg. Chim. Acta,* 2014, **416**, 13; (c)X. F. Zhu, N. Wang, X. Y. Xie, R. B. Hou, D. F. Zhou, Y. F. Li, J. Hu, X. Y. Li, H. Liu and W. Nie, *RSC Adv.,* 2014, **4**, 15816; (d)S. Yuan, S. S. Liu and D. Sun, *CrystEngComm,* 2014, **16**, 1927; (e)J. Y. Li, Z. P. Ni, Z. Yan, Z. M. Zhang, Y. C. Chen, W. Liu and M. L. Tong, *CrystEngComm,* 2014, **16**, 6444; (f)M. Ahmad, R. Katoch, A. Garg and P. K. Bharadwaj, *CrystEngComm.,* 2014, **16**, 4766; (g)K. K. Bisht and E. Suresh, *Cryst. Growth Des.,* 2013, **13**, 664.

[18](a)L. J. Li, X. L. Wang, K. Z. Shao, Z. M. Su and Q. Fu, *Inorg. Chim. Acta.,* 2012, **392**, 77; (b)L. J. Li, C. Qin, X. L. Wang, S. Wang, L. Zhao, G. S. Yang, H. N. Wang, G. Yuan, K. Z. Shao and Z. M. Su, *CrystEngComm.,* 2012, **14**, 124.

[19](a)J. X. Yang, Y. Y. Qin, J. K. Cheng and Y. G. Yao, *Cryst. Growth Des.,* 2014, **14**, 1047; (b)A. Beheshti, A. Lalegani, G. Bruno and H. A. Rudbari, *J. Mol. Struct.,* 2014, **1071**, 18; (c)V. Nobakht, A. Besheshti, D. M. Proserpio, L. Carlucci and C. T. Abrahams, *Inorg. Chem. Acta.,* 2014, **414**, 217; (d)M. L. Han, Y. P. Duan, D. S. Li, G. W. Xu, Y. P. Wu and J. Zhao, *Dalton Trans.,* 2014, **43**, 17519; (e)G. B. Yang and Z. H. Sun, *Inorg. Chem. Commun.,* 2013, **29**, 94; (f)A. Beheshti, A. Lalegani, G. Bruno and H. A. Rudbari, *J. Mol. Struct.,* 2013, **1051**, 244; (g)X. H. Lou, C. Xu, H. M. Li, Z. J. Zhang and H. Zhang, *J. Inorg. Organomet. Polym.,* 2013, **23**, 659; (h)Y. Xu, Y. X. Che and J. M. Zheng, *Z. Anorg. Allg. Chem.,* 2012, **638**, 698; (i)X. J. Li, X. F. Guo, X. L. Weng and S. Lin, *CrystEngComm.,* 2012, **14**, 1412; (j)L. F. Ma, M. L. Han, J. H. Qin, L. Y. Wang and M. Du, *Inorg. Chem.,* 2012, **51**, 9431;

[20](a)H. Wang, X. Y. Yang, Y. Q. Ma, W. B. Cui, Y. H. Li, W. G. Tian, S. Yao, Y. Gao, S. Dang and W, Zhu, *Inorg. Chim. Acta,* 2014, **416**, 63; (b)K. H. Wang and E. J. Gao, *J. Coord. Chem.,* 2014, **67**, 563; (c)F. L. Hu, S. L. Wang, B. Wu, H. Yu, F. Wang and J. P. Lang, *CrystEngComm,* 2014, **16**, 6354; (d)C. L. Zhang, H. Hao, Z. Z. Shi and H. G. Zheng, *CrtstEngComm,* 2014, **16**, 5662; (e)W. T. Yang, S. Dang, H. Wang, T. Tian, Q. J. Pan and Z. M. Sun, *Inorg. Chem.,* 2013, **52**, 12394; (f)F. L. Hu, W. Wu, P. Liang, Y. Q. Gu, L. G. Zhu and J. P. Lang, *Cryst. Growth Des.,* 2013, **13**, 5050; (g)Y. Qi, Y. H. Li and Y. Wang, *Z. Anorg. Allg. Chem.,* 2013, **639**, 2258; (h)L. Chen, L. Zhang, S. L. Li, Y. Q. Qiu, K. Z. Shao, X. L. Wang and Z. M. Su, *CrystEngComm,* 2013, **15**, 8214; (i)F. L. Hu, Y. Ma, Y. Q. Gu, L. G. Zhu, S. L. Yang, H. Wei and J. P. Lang, *CrystEngComm,* 2013, **15**, 9553.

[21](a)J. S. Hu, X. J. Zhang, X. W. Cai, L. X. Sun, W. H. Zhang, J. J. Shi, X. M.Zhang, H. L. Xing and J. He, *Chinese J. Inorg. Chem.,* 2014, **30**, 654; (b)J. S. Hu, X. Zhuo, X. H. Liu, H. L. Xing, J. He and H. G. Zheng, *Inorg. Chem. Commun.,* 2013, **33**, 15; (c)J. S. Hu, L. F. Huang, X. Q. Yao, L. Qin, Y. Z. Li, Z. J. Guo, H. G. Zheng and Z. L. Xue, *Inorg. Chem.,* 2011, **50**, 2404; (d)X. L. Mu, *Acta Crystallogr.,* 2011, **E67**, m166; (e)J. S. Hu, Y. J. Shang, X. Q. Yao, L. Qin, Y. Z. Li, Z. J. Guo, H. G. Zheng and Z. L. Xue, *Cryst. Growth Des.,* 2010, **10**, 4135.
[22](a)D. S. Li, Y. P. Wu, J. Zhao, J. Zhang and J. Y. Lu, *Coord. Chem. Rev.*, 2014, **261**, 1; (b)M. Du, C. P. Li, C. S. Liu and S. M. Fang, *Coord. Chem. Rev.*, 2014, **257**, 1282; (c) D. S. Li, J. Zhao, Y. P. Wu, B. Liu, L. Bai, K. Zou and M. Du, *Inorg. Chem.*, 2013, **52**, 8091.
[23](a)H. D. Guo, X. M. Guo, H. Y. Zou, Y. J. Qi and R. Z. Chen, *CrystEngComm*, 2014, **16**, 2176; (b) X. M. Guo, H. D. Guo, H. Y. Zou, Y. J. Qi and R. Z. Chen, *CrystEngComm*, 2013, **15**, 9112.
[24]B. Liu, Q. Zhang, H. Ding, G. Hu, Y. Du, C. Wang, J. Wu, S. Li, H. Zhou, J. Yang and Y. Tian, *Dyes and Pigm.*, 2012, ***95***, 149; (b)J. L. Zhou, Y. Y. Wang, M. J. Zhou, L. Qin, M. D. Zhang, Q. X. Yang and H. G. Zheng, *Inorg. Chem. Commun*., 2014, **40**, 148.
[25](a)G. M. Sheldrick, SHELXS-97, Programs for X-ray Crystal Structuer Solution, University of Göttingen, Germany, 1997; (b) G. M, Sheldrick, *Acta Crystallog A*, 2008, **64**, 112.
[26]G. M. Sheldrick, SHELXL-97, Programs for X-ray Crystal Structuer Refinement, University of Göttingen, Göttingen, Germany, 1997.
[27]L. Qin, J. S. Hu, Y. Z. Li and H. G. Zheng, *Cryst.Growth Des.,* 2011, ***11***, 3115.
[28]J. Xu, X. Q. Yao, L. F. Huang, Y. Z. Li and H. G. Zheng, *CrystEngComm.*, 2011, **16**, 857.
[29](a) M. D. Allendorf, C. A. Bauer, R. K. Bhakta and R. J.T. Houk, Chem. Soc. Rev., 2009, **38**, 1330; (b) H. D. Guo, X.M. Guo, S. R. Batten, J. F. Song, S. Y. Song, S. Dang, G.L. Zheng, J. K. Tang and H. J. Zhang, Cryst. Growth Des., 2009, **9**, 1394.

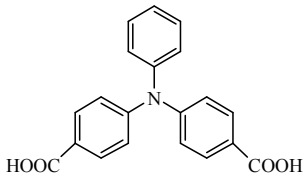

4,4'-(phenylazanediyl)dibenzoic acid (H_2L)

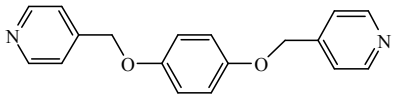

1,4-bis(pyridin-4-ylmethoxy)benzene (bpmb)

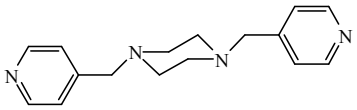

1,4-bis(pyridin-4-ylmethl)piperazine (bpmp)

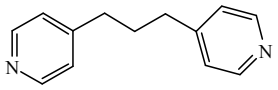

1,3-bis(4-pyridyl)propane (bpp)

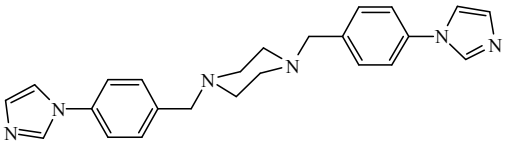

1,4-bis(4-(1H-imidazol-l-yl)benzyl)piperazine (bibpa)

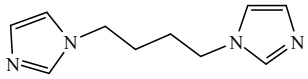

1,4-bis(imidazolyl)butane (bib)

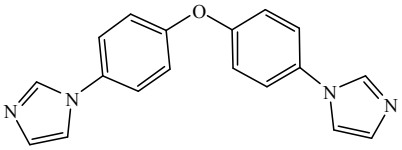

4,4'-bis(imidazol-1-yl)dipheny ether (bidpe)

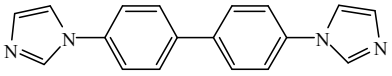

4,4'-bis(imidazol-1-yl)biphenyl (bibp)

Scheme 1 Molecular structure of ligands.

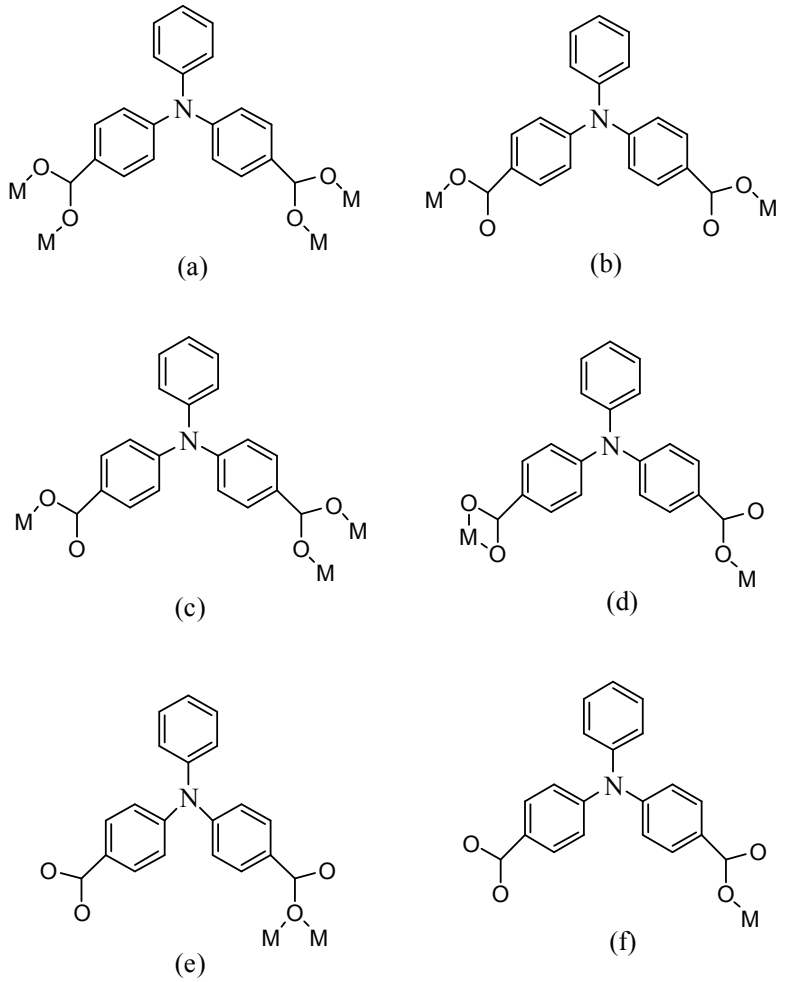

Scheme 2 Crystallographically established coordination modes of the carboxylic groups in compounds **1-9**.

Table 1 Crystal and Structure Refinement Data for Compounds **1-9**.

Compound	**1**	**2**	**3**	**4**	**5**
CCDC No.	1058540	1058542	1058543	1058545	1058546
Formula	$C_{28}H_{23}N_3O_7Zn$	$C_{76}H_{54}N_{10}O_9Zn_2$	$C_{33}H_{27}N_3O_8Zn$	$C_{76}H_{54}N_{10}O_{12}Zn_2$	$C_{136}H_{98}N_{10}O_{28}Zn_5$
Fw	578.86	1382.03	658.95	1414.03	2647.09
Crystal system	Monoclinic	Monoclinic	Monoclinic	Triclinic	Orthorhombic
Space group	*C*2/*c*	$P2_1/n$	*C*2/*c*	$P\bar{1}$	$P2_12_12$
a/Å	29.139(18)	9.3089(6)	21.483(2)	14.3887(18)	14.2821(17)
b/Å	8.292(6)	50.079(3)	18.7268(19)	15.538(2)	42.185 (2)
c/Å	22.798(15)	14.5655(9)	21.298(3)	17.003(2)	9.6119(5)
α(°)	90.00	90.00	90.00	87.718(3)	90.00
β(°)	94.970(11)	107.9530(10)	118.853 (2)	65.714(2)	90.00
γ(°)	90.00	90.00	90.00	76.845(3)	90.00
V(Å^3)	5488(6)	6459.5(7)	7504.5(15)	3367.8(7)	5791.0
Z	8	4	8	2	2
D_c(g cm^{-3})	1.401	1.421	1.166	1.410	1.518
μ/mm^{-1}	0.945	0.812	0.701	0.785	1.106
F(000)	2384	2848	2720	1473	2716
Total,unique data	17578, 6927	39615, 15572	27489, 9365	25205, 16823	40776, 14151
R_{int}	0.0431	0.0559	0.0423	0.0650	0.0766
Observed data[$I>2\sigma(I)$]	4566	7850	5357	6927	8560
Nrcf,Npar	6927, 337	15572, 869	9365, 394	16823, 896	14151, 807
R_1, *wR2*[$I>2\sigma(I)$]	0.0527/0.1270	0.0610, 0.1374	0.0611, 0.1900	0.0798, 0.1798	0.0623, 0.1461

R_1, wR_2 (all data)	0.0936/0.1458	0.1526, 0.1802	0.1030, 0.2218	0.2109, 0.2577	0.1380, 0.1903
s	1.049	1.038	01.013	0.964	1.017
Largest diff. peak and hole /e·Å^{-3}	0.990, -0.523	0.377, -0.556	1.095, -0.487	0.699, -0.810	1.081, -1.367

Compound	**6**	**7**	**8**	**9**
CCDC No.	1058547	1058548	1058550	1058551
Formula	$C_{92}H_{84}N_{16}O_{13}Zn_2$	$C_{58}H_{44}N_4O_{10}Zn$	$C_{30}H_{26}N_5O_4Zn$	$C_{44}H_{36}N_7O_6Zn$
Fw	1752.49	1020.38	585.93	824.17
Crystal system	Triclinic	Monoclinic	Orthorhombic	Monoclinic
Space group	$P\bar{1}$	$C2/c$	$Pbca$	$P2_1/c$
a/Å	10.6126(14)	28.327(4)	16.668(6)	14.7273(16)
b/Å	13.0570(16)	6.0289(8)	16.256(6)	34.677(4)
c/Å	18.873(2)	29.409(4)	28.596(10)	8.2504(9)
α(°)	77.782(2)	90.00	90.00	90.00
β(°)	81.567(2)	107.892(3)	90.00	104.498(2)
γ(°)	73.826(2)	90.00	90.00	90.00
V	2444.1(5)	4779.7(11)	7748(5)	4079.3(8)
Z(Å^3)	1	4	8	4
D_c (g cm^{-3})	1.191	1.418	1.005	1.342
μ/mm^{-1}	0.555	0.582	0.666	0.659
F(000)	912	2112	2424	1708
Total,unique data	13712, 9520	16998, 5910	54960, 9851	24362, 7763
R_{int}	0.0329	0.0845	0.1438	0.0700
Observed data[I>2σ(I)]	5520	3163	3769	5027
N_{rcf},N_{par}	9520, 541	5910, 330	9851, 361	7763, 473
R_1, wR_2[I>2σ(I)]	0.0766, 0.2134	0.0554, 0.1234	0.0611, 0.1328	0.0968, 0.2404
R_1, wR_2 (all data)	0.1370, 0.2394	0.1328, 0.1666	0.1700, 0.1617	0.1492, 0.661
s	1.019	1.003	0.840	1.119
Largest diff. peak and hole /e·Å^{-3}	0.912, -0.338	0.397, -0.554	0.540, -0.439	2.581, -0.661

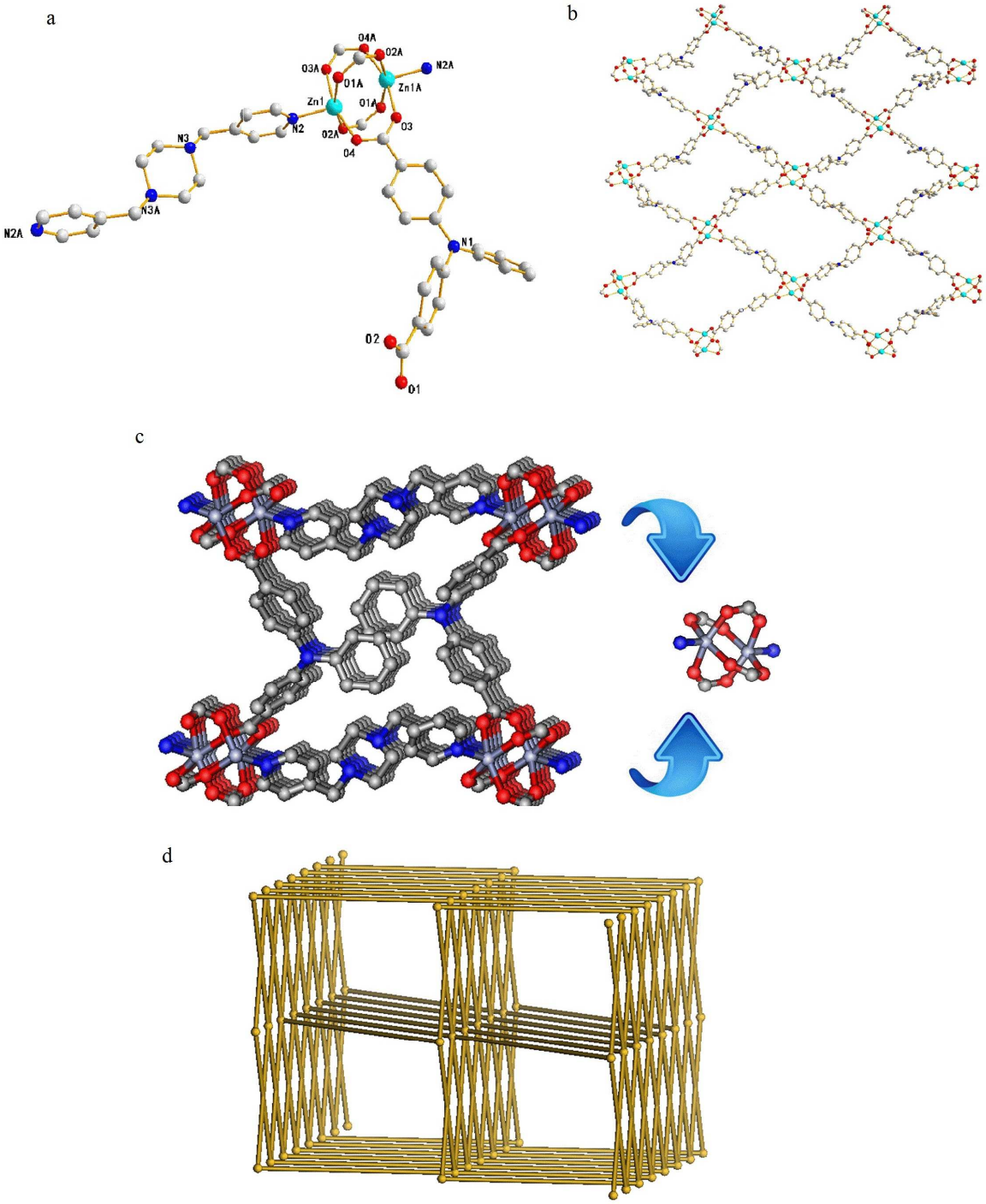

Fig. 1 (a) Coordination environment of the Zn(II) ions in compound **1**. The hydrogen atoms are omitted for clarity. Symmetry codes: #1= -x+1.5, -y-0.5, -z+1; #2=-x+2, y-1, -z+1.5; #3= x, -y, z+0.5; #4=-x+2, -y+1, -z+1; #5=-x+2, y+1, -z+1.5; #6= x, -y, z-0.5. (b) views of 2D net structure. (c) views of the 3D framework. (d) The $\{4^4 \cdot 6^{10} \cdot 8\}$ topology net.

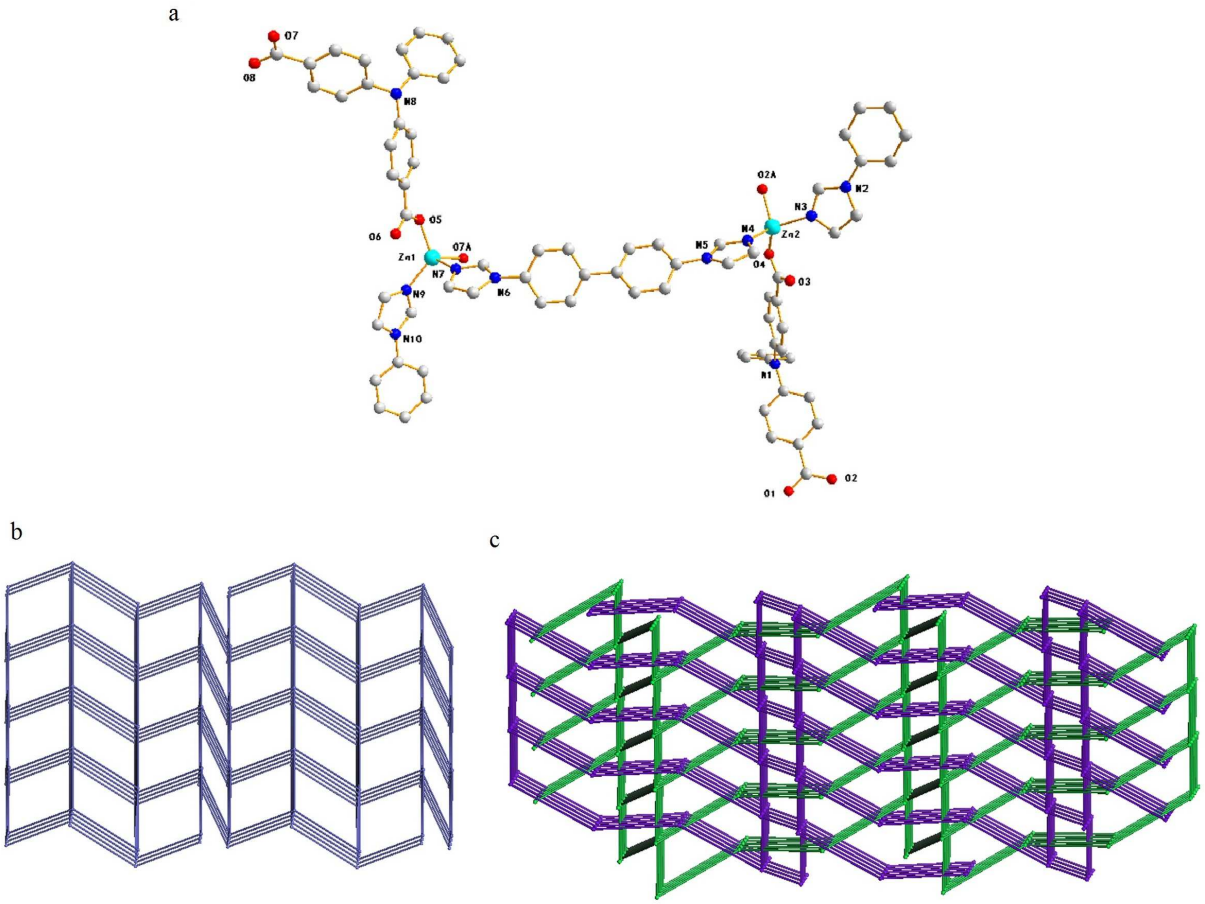

Fig. 2 (a) Coordination environment of the Zn(II) ions in compound **2**. The hydrogen atoms are omitted for clarity. Symmetry codes: #1=x, y, z+1; #2=x-1, y, z-1; #3=x+1, y, z+1; #4=x, y, z-1; #5=-x+1, -y, -z; #6=-x-1, -y+1, -z+1. (b) views of 3D framework structure. (c) Schematic view of the two-fold interpenetrating framework.

5

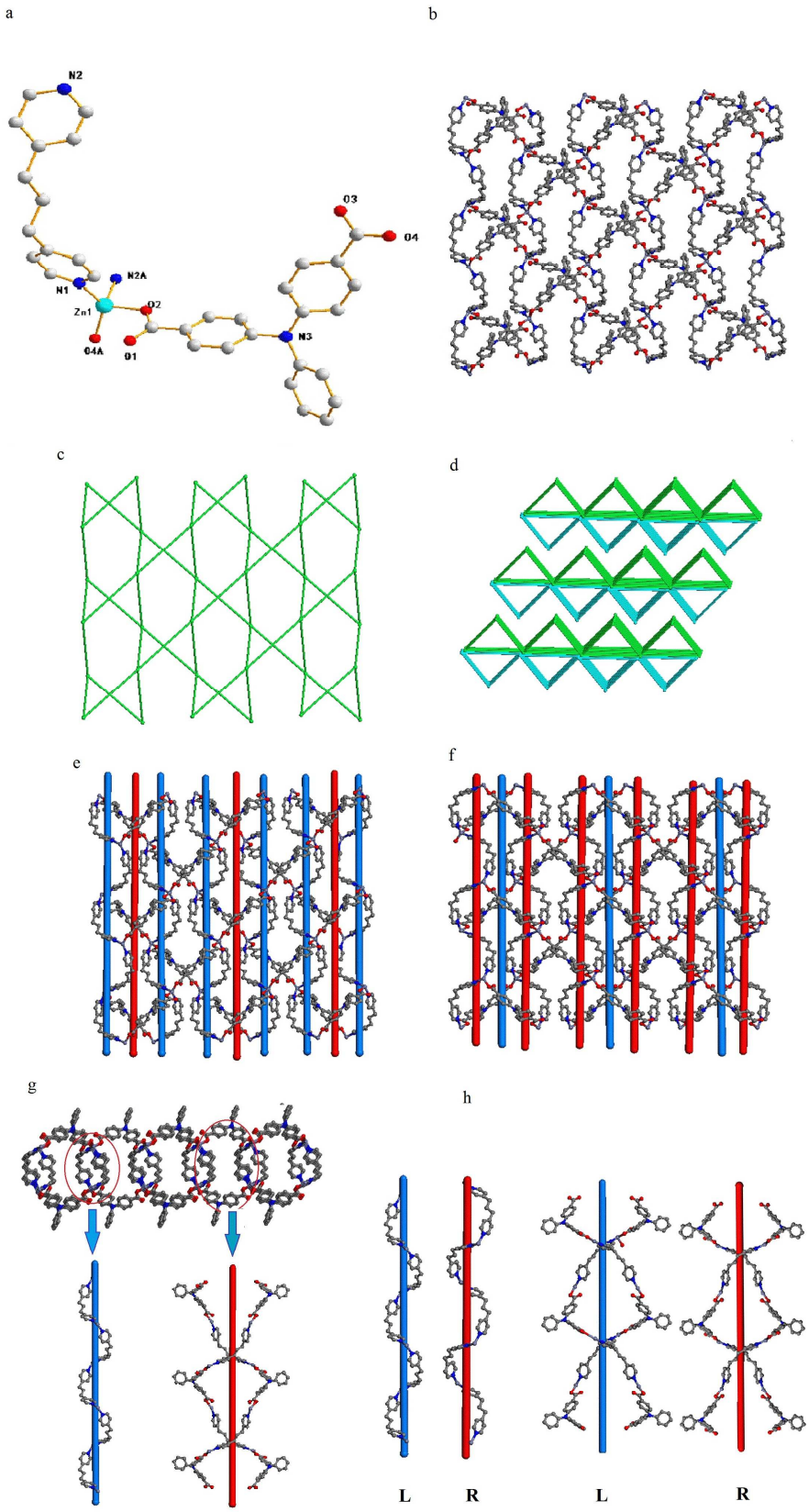

Fig. 3 (a) Coordination environment of the Zn(II) ions in compound **3**. The hydrogen atoms are omitted for clarity. Symmetry codes: #1= x+, y-0.5, z; #2= -x+1.5, y-0.5, -z+0.5; #3=x-0.5, y+0.5, z; #4=-x+1.5, y+0.5, -z+0.5. (b, c) views of 2D net structure. (d) view of the sheets are stacked in ABAB fashion, a 3D framework. (e, f, g) views of the helical chains with uniform or opposite hardness. (h) views of the helical chains in the (4,4) layer.

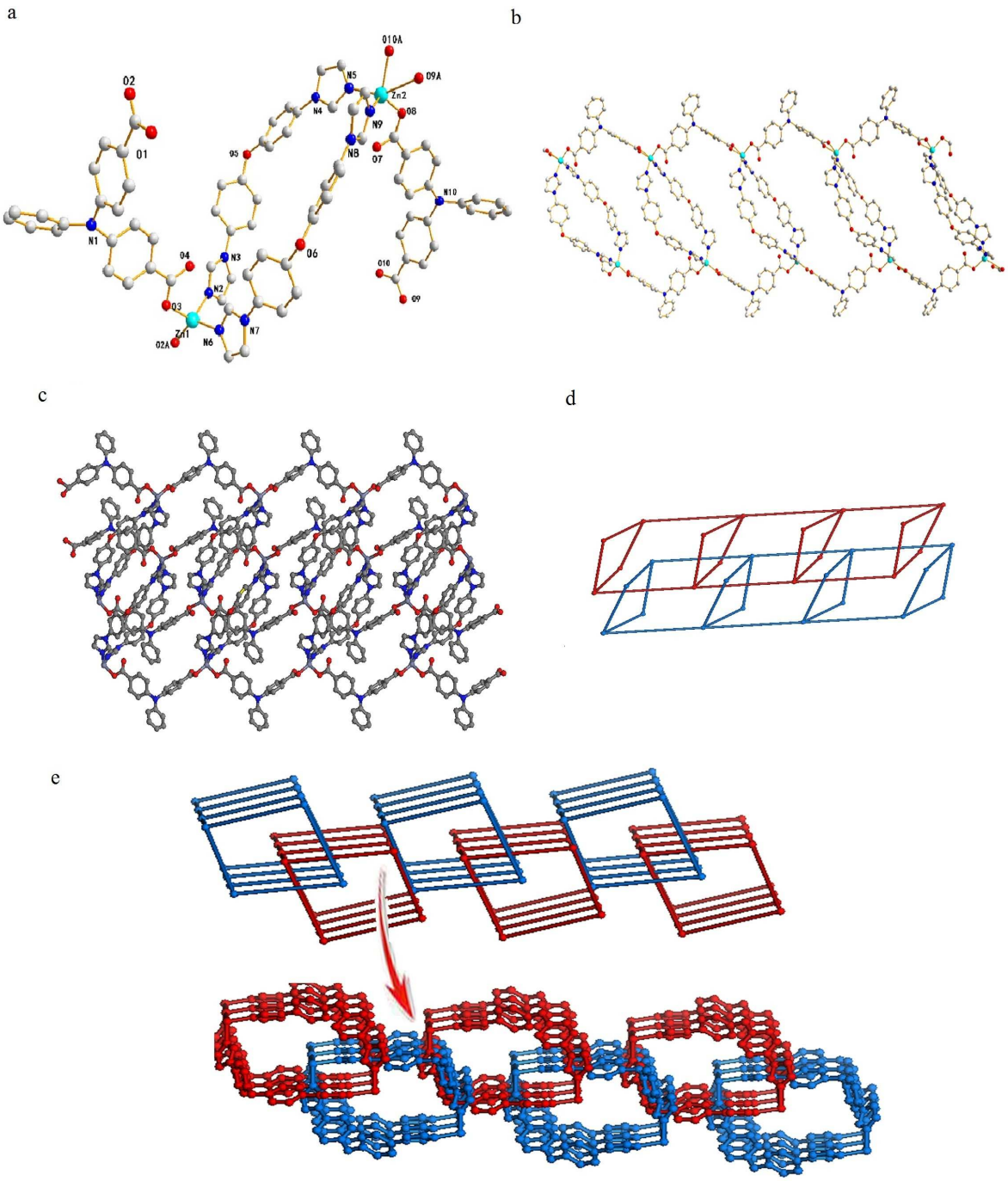

Fig. 4 (a) Coordination environment of the Zn(II) ions in compound **4**. The hydrogen atoms are omitted for clarity. Symmetry codes: #1=x-1, y, z; #2= x+1, y, z. (b) views of the 1D chain. (c, d) views of 2-fold interpenetrated 1D chain. (e) views of the 2D sheets.

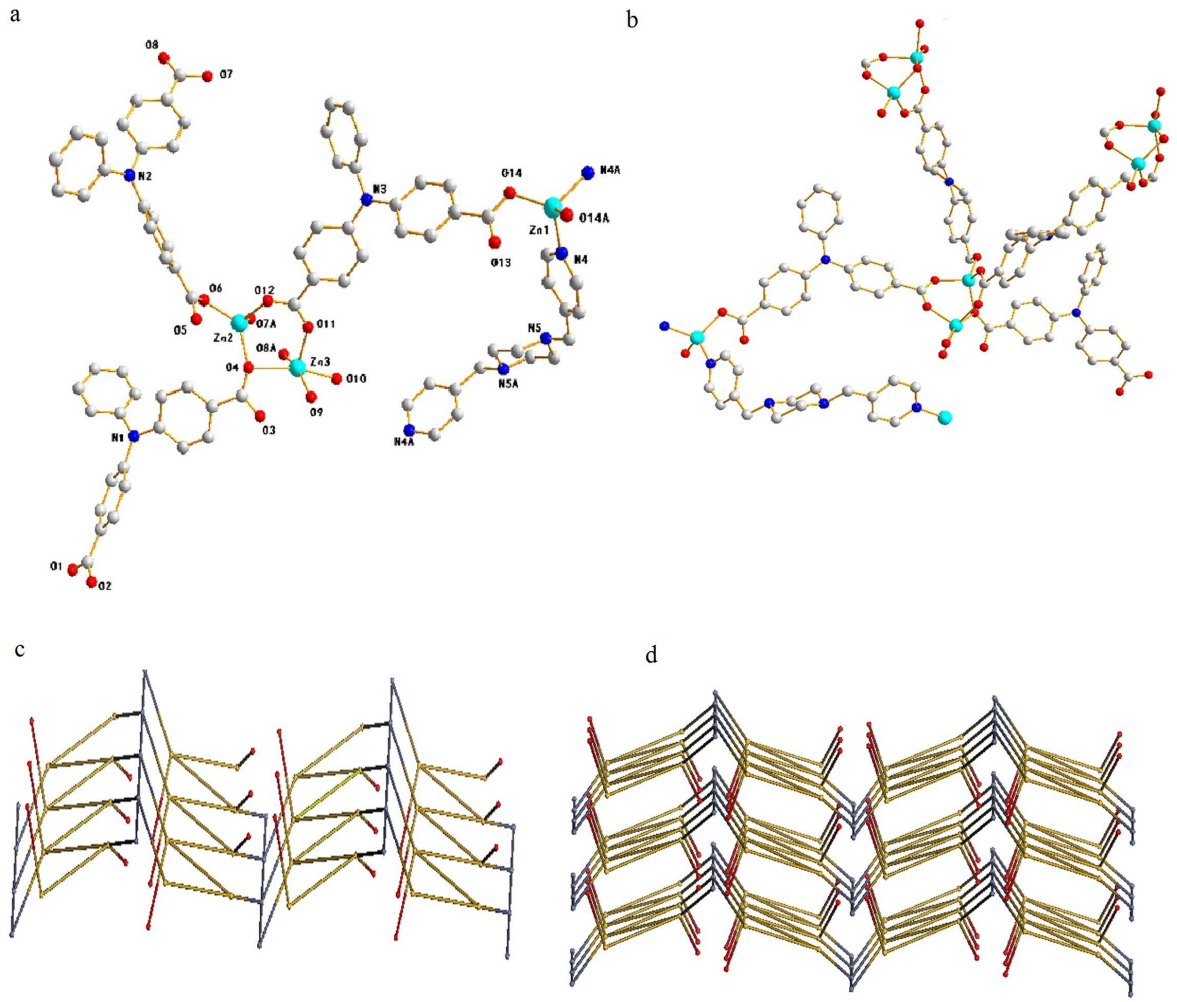

Fig. 5 (a) Coordination environment of the Zn(II) ions in compound **5**. The hydrogen atoms are omitted for clarity. Symmetry codes: #1=-x+1, -y, z; #2= x+0.5, -y+0.5, -z+2; #3=-x+2, -y, z; #4=x-0.5, -y+0.5, -z+2. (b) views of the 1D chain. (c) views of 2D wave-like sheets. (e) views of the 3D framework.

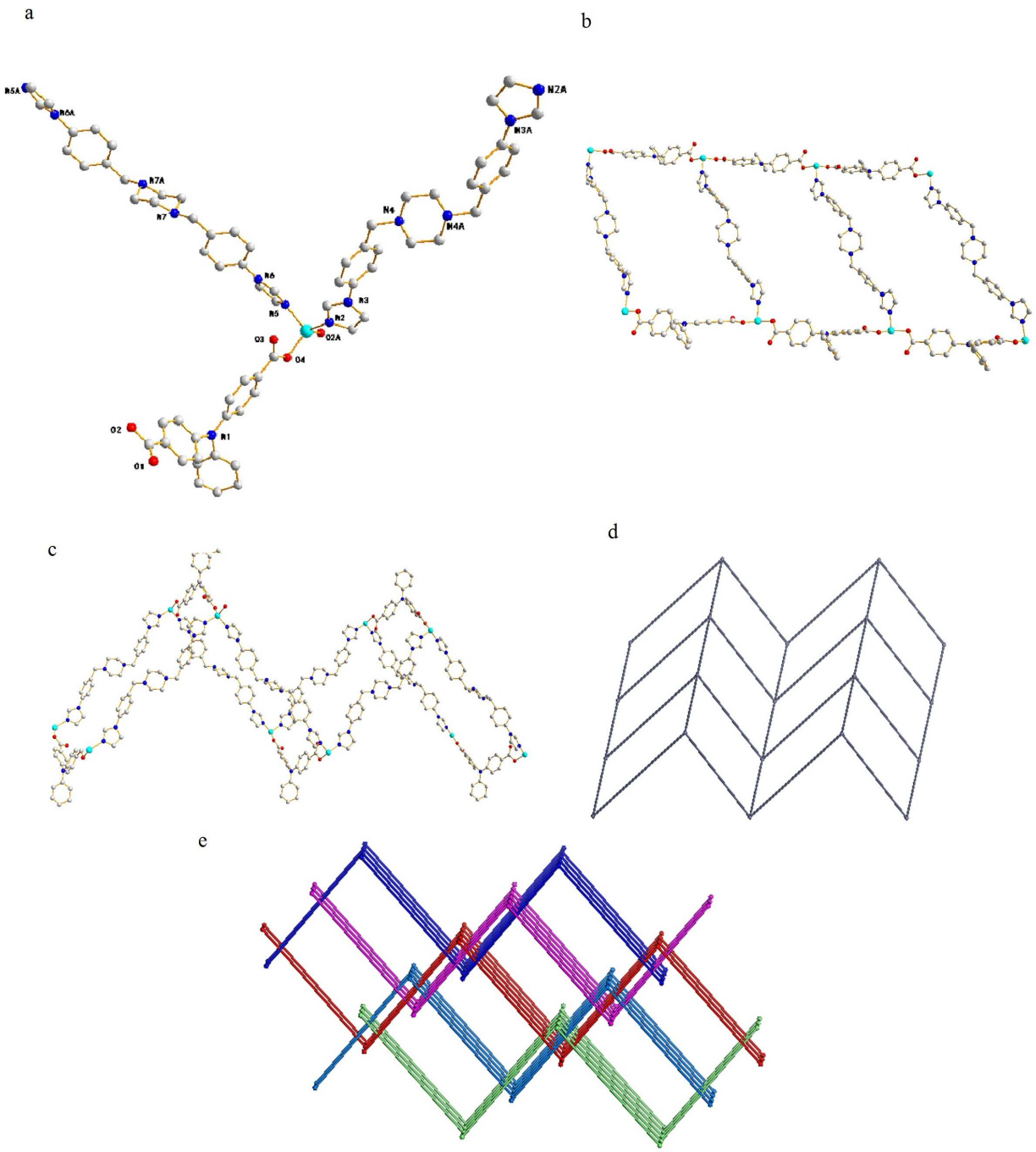

Fig. 6 (a) Coordination environment of the Zn(II) ions in compound **6**. The hydrogen atoms are omitted for clarity. Symmetry codes: #1=-x+1, -y, -z+2; #2=-x+2, -y+2, -z+1; #3=x-1, y+1, z; #4=x+1, y-1, z; #5=-x+1, -y+1, -z. (b, c, d) views of 2D wave-like sheets. (e) Schematic view of the 5-fold interpenetrating framework.

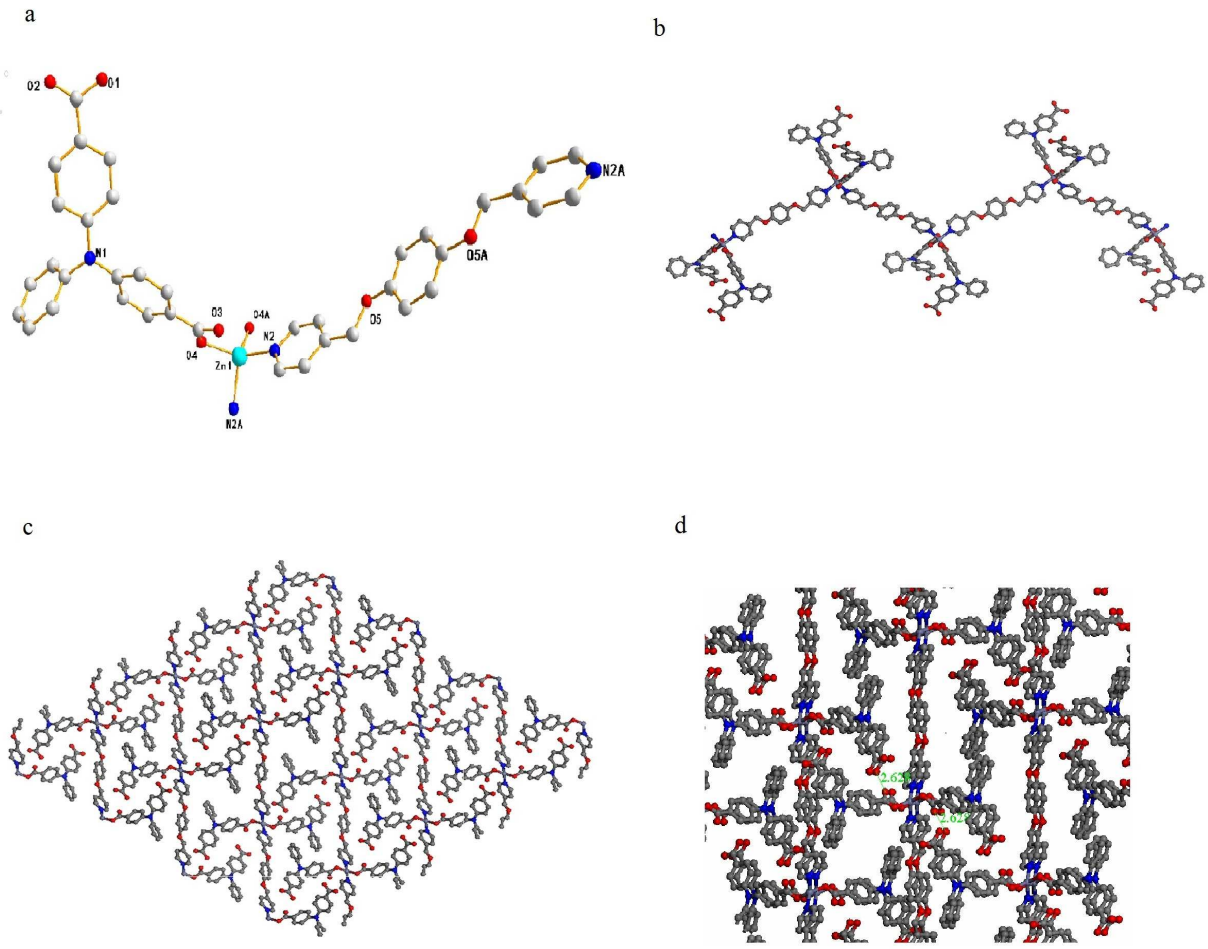

Fig. 7 (a) Coordination environment of the Zn(II) ions in compound **7**. The hydrogen atoms are omitted for clarity. Symmetry codes: #1=-x+1.5, -y+3.5, -z+2; #2=-x+1, y, -z+1.5. (b) views of the 1D chain. (c) views of 2D sheets. (d) views of the distances between two O atoms in adjoining layers.

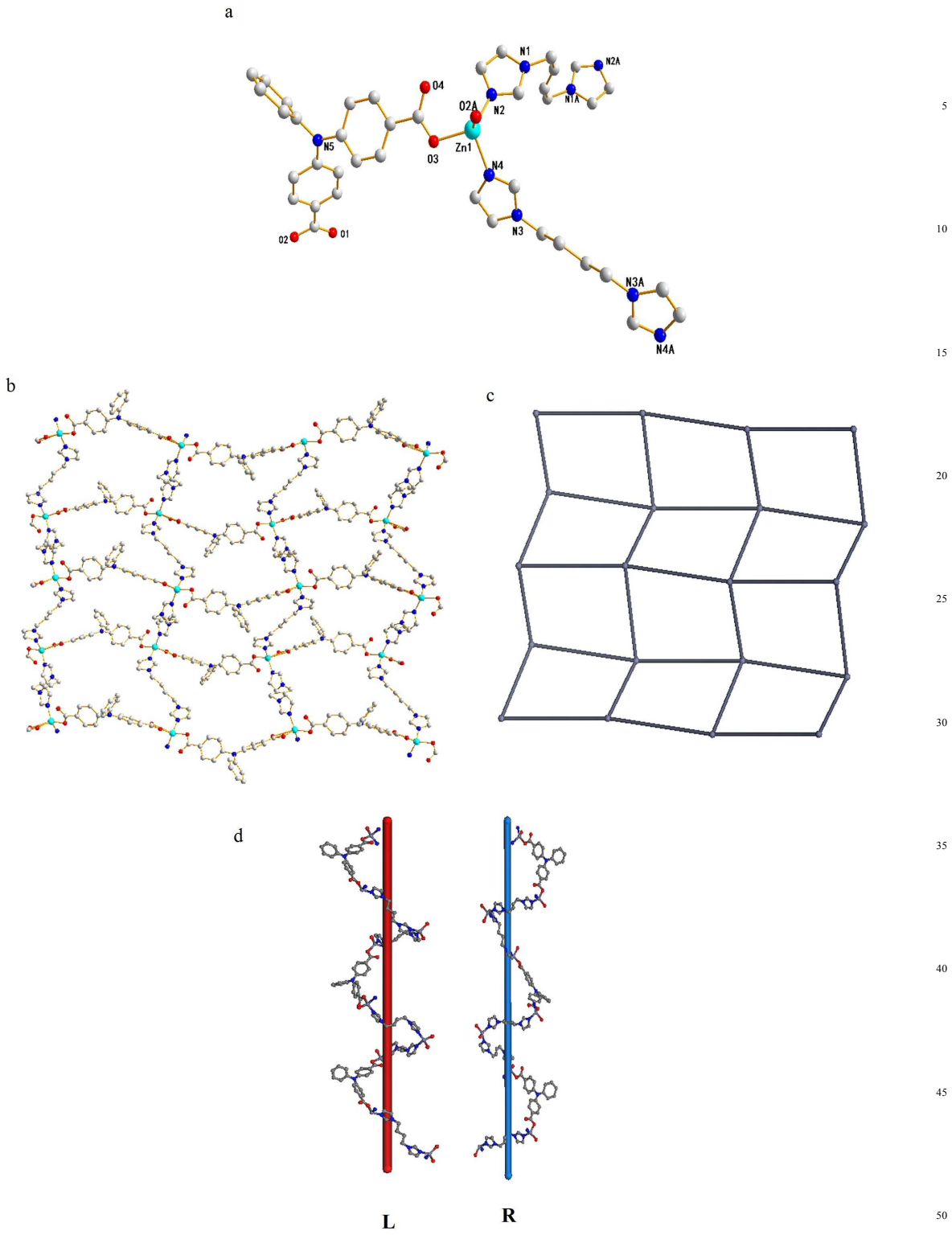

Fig. 8 (a) Coordination environment of the Zn(II) ions in compound **8**. The hydrogen atoms are omitted for clarity. Symmetry codes: #1=-x+2, -y, -z; #2= -x+2, -y+1, -z; #3=x, -y+0.5, z-0.5; #4=x, -y+0.5, z+0.5, #5=-x+1, y-0.5, -z-0.5; #6=-x+1, y+0.5, -z-0.5. (b, c) views of 2D net structure. (d) A view of the helical chains.

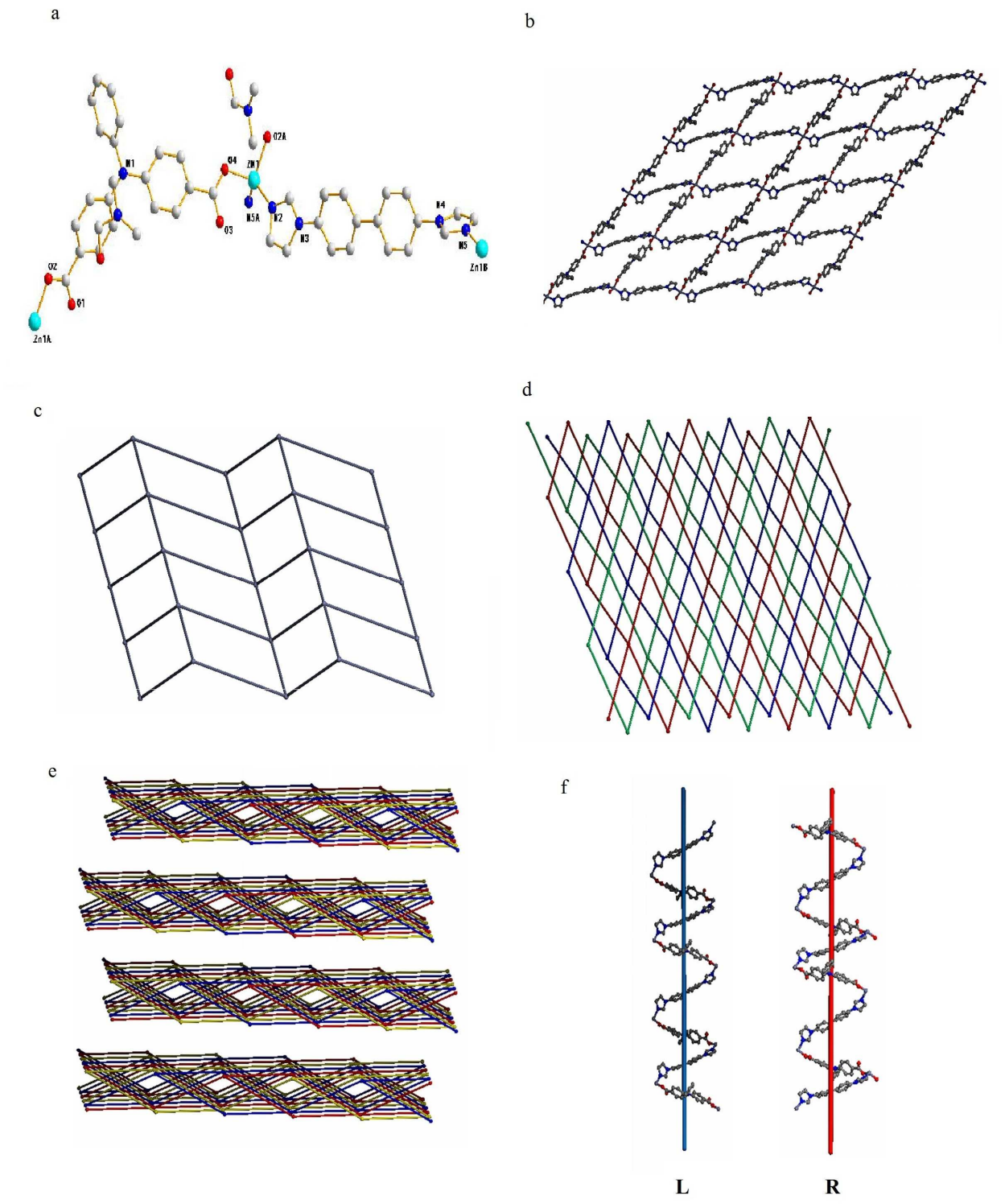

Fig. 9 (a) Coordination environment of the Zn(II) ions in compound **9**. The hydrogen atoms are omitted for clarity. Symmetry codes: #1=x+1, y, z+1; #2= x-1, -y+0.5, z+0.5; #3=x+1, -y+0.5, z-0.5; #4=x-1, y, z-1. (b, c) views of 2D net structure. (d) Schematic view of the three-fold interpenetrating sheets. (e) The sheets are stacked in ABAB fashion and form a 3D framework. (f) A view of the helical chains.

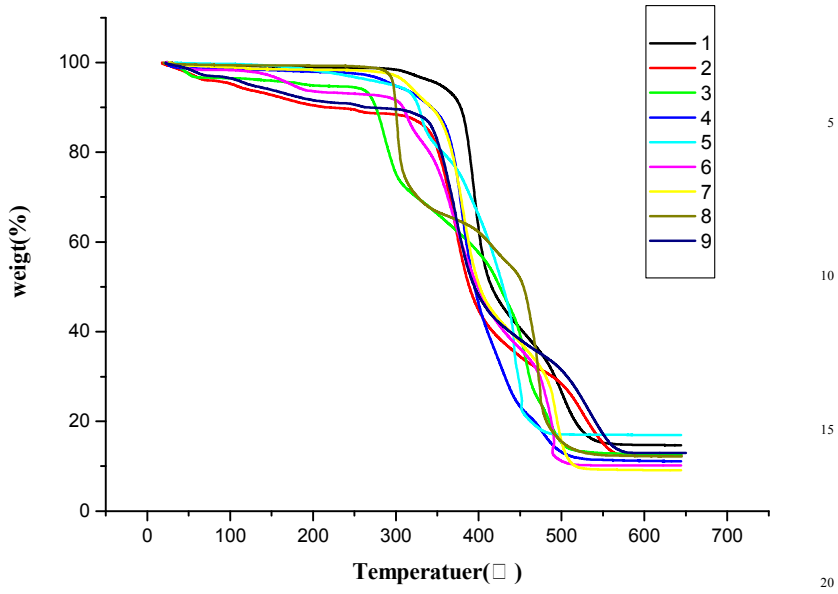

Fig. 10 The TGA diagrams of complexes **1-9**.

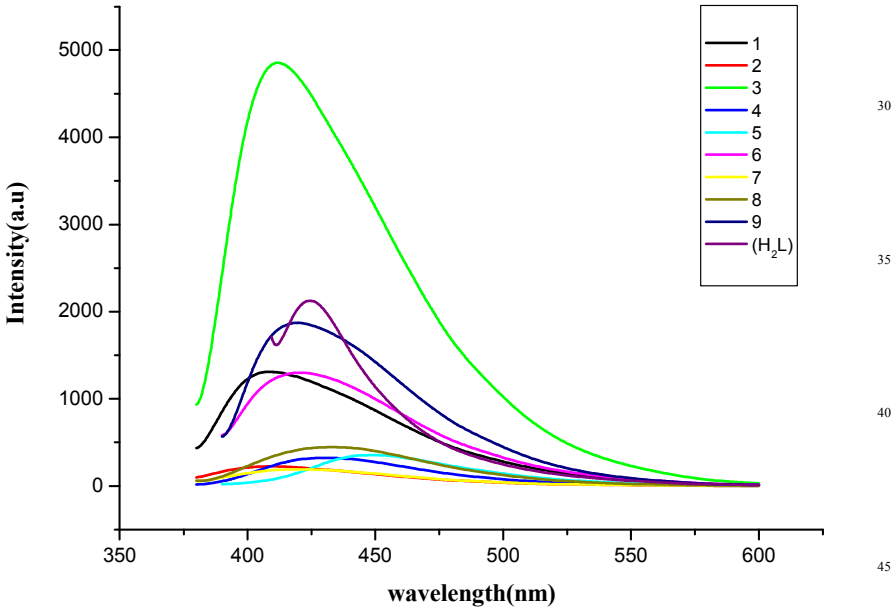

Fig. 11 The solid-state photoluminescent spectra of **1-9** and H_2L at room temperature.